Tectonophysics 584 (2013) 23–42

Contents lists available at SciVerse ScienceDirect

Tectonophysics

journal homepage: www.elsevier.com/locate/tecto

Characteristics of the fault-related rocks, fault zones and the principal slip zone in the Wenchuan Earthquake Fault Scientific Drilling Project Hole-1 (WFSD-1)

Haibing Li [a,b,*], Huan Wang [a,b], Zhiqin Xu [a,b], Jialiang Si [a,b], Junling Pei [a,c], Tianfu Li [a,b], Yao Huang [d], Sheng-Rong Song [e], Li-Wei Kuo [e], Zhiming Sun [a,c], Marie-Luce Chevalier [a,b], Dongliang Liu [a,b]

[a] State Key Laboratory of Continental Tectonic and Dynamics, Beijing 100037, China
[b] Institute of Geology, Chinese Academy of Geological Sciences, No.26, Baiwanzhuang Road, Beijing 100037, China
[c] Institute of Geomechanics, Chinese Academy of Geological Sciences, Beijing 100081, China
[d] No.6 brigade of Jiangsu Geology & Mineral Resources Bureau, Lianyungang, Jiangsu, 222300, China
[e] Department of Geosciences, National Taiwan University, Taipei, China

ARTICLE INFO

Article history:
Received 2 September 2011
Received in revised form 12 August 2012
Accepted 14 August 2012
Available online 24 August 2012

Keywords:
Wenchuan earthquake fault scientific drilling project (WFSD)
Yingxiu–Beichuan fault zone
Fault-related rocks
Principal slip zone (PSZ)
Wenchuan earthquake
WFSD-1

ABSTRACT

Scientific drilling in active faults after a large earthquake is ideal to study earthquake mechanisms. The Wenchuan earthquake Fault Scientific Drilling project (WFSD) is an extremely rapid response to the 2008 Ms 8.0 Wenchuan earthquake, which happened along the Longmenshan fault, eastern margin of the Tibetan Plateau. In order to better understand the fault mechanism and the physical and chemical characteristics of the rocks, the WFSD project will eventually drill 5 boreholes along the two main faults. This paper focuses on the first hole (WFSD-1), which started just 178 days after the earthquake, down to a final depth of 1201.15 m. Petrological and structural analyses of the cores allowed the identification of fault-related rocks in the Yingxiu–Beichuan fault (fault gouge, cataclasite, and fault breccia), and the Principle Slip Zone (PSZ) location of the Wenchuan earthquake was determined.

We found 12 fault zones in the entire core profile, with at least 10, including the Yingxiu–Beichuan fault zone, with a multiple cores structure and minimum width of ~100 m. The co-seismic slip plane of the Wenchuan earthquake at depth (corresponding to the Yingxiu–Beichuan fault zone at the outcrop), as well as its PSZ, was expected to be located at the bottom of the fault zone (at 759 m-depth). Instead, it was found at ~590 m-depth with 1 cm-wide fresh fault gouge, as determined by logging data such as temperature, natural gamma ray, p-wave velocity and resistivity, combined with the fresh appearance, magnetic susceptibility, and microstructure of the gouge. The Wenchuan earthquake slip plane has a dip angle of ~65°, showing the high-angle thrust feature. The distribution of fault gouge with several meters thick, the location of the Wenchuan earthquake's PSZ and the thickness of fresh gouge all imply a correlation between the width of the fault zone and the number of seismic events.

1. Introduction

The May 2008, Ms 8.0 Wenchuan earthquake occurred in the transition zone between the Tibetan Plateau and the Sichuan Basin, within the Longmenshan, yielding 270 and 80 km-long co-seismic surface ruptures along the Yingxiu–Beichuan and Anxian–Guanxian faults, respectively (Fu et al., 2011; Li et al., 2008; Liu-Zeng et al., 2010; Xu et al., 2009). This large earthquake caused disastrous damages but stimulated numerous research on active faults and their tectonic framework along the SW margin of the Tibetan Plateau. This study aims at helping to understand earthquake mechanisms capable of generating such catastrophic events.

In order to better understand the mechanical, physical and chemical characteristics of the faults that ruptured during the Wenchuan earthquake, the two main strands of the fault are currently being drilled under the auspices of the Wenchuan earthquake Fault Scientific Drilling project (WFSD), funded by the Chinese government alone.

Drilling in active fault zones, especially post-large earthquakes, provides important information on the physical characteristics and the formation of these highly-deformed geological features (Brodsky et al., 2009; Z.Q. Xu et al., 2008; Zoback et al., 2007) and will shed light on the geology of the fault zones and allow to correlate their structure and mineralogy with their seismological behavior during recent earthquakes (Boullier, 2011). The first drilling project following a large earthquake started after the 1995 Kobe earthquake (Nojima Fault Probe Project) (Oshiman et al., 2001). A few years later, the Taiwan Chelungpu fault Drilling Project (TCDP) started after the 1999 Taiwan Chi-Chi earthquake (e.g. Ma et al., 2006; Song et al., 2007).

* Corresponding author at: Institute of Geology, Chinese Academy of Geological Sciences, No.26, Baiwanzhuang Road, Beijing 100037, People's Republic of China. Tel.: +86 10 68990581; fax: +86 10 68994781.
E-mail address: lihaibing06@yahoo.com.cn (H. Li).

0040-1951/$ – see front matter © 2012 Elsevier B.V. All rights reserved.
http://dx.doi.org/10.1016/j.tecto.2012.08.021

The Wenchuan Fault Scientific Drilling project (WFSD) is the third drilling project into fault zones. The first borehole drilling (WFSD-1) started just 178 days after the earthquake, on November 6th 2008, and was completed by July 12th 2009, with a total depth of 1201.15 m and 95.4% of core recovery. It represents the most rapid response project to study a large earthquake and its aftershocks. Five boreholes ranging from 550 m to 3400 m-depth will ultimately be drilled along the Yingxiu–Beichuan and Anxian–Guanxian faults, targeting the locations of maximum co-seismic slip. WFSD-1 and WFSD-2, with depths of 1201.15 and 2283.56 m respectively, are located on the hanging wall of the southern Yingxiu–Beichuan fault zone in Bajiaomiao village, where the largest vertical displacement was about 6 m (Fu et al., 2011; Li et al., 2008; Liu-Zeng et al., 2010; Xu et al., 2009). The two other boreholes (WFSD-3P and WFSD-3) were drilled on the hanging wall of the Anxian–Guanxian fault in Qingquan village, Mianzhu City, with depths of 551.65 and 1502.18 m respectively (the maximum vertical displacement was about 4 m). WFSD-4 started to be drilled on August 6th 2012 and will reach a depth of about 3400 m. It is located along the northern part of the Yingxiu–Beichuan fault zone in the Nanba area, where the observed vertical displacement was about 1.5 to 2.5 m (Fu et al., 2011; Li et al., 2008, 2010a,c; Liu-Zeng et al., 2010; Xu et al., 2009), and the dextral displacement was ~2 m (Li et al., 2008; Li et al., 2010a,c; Xu et al., 2009). The geological, chemical, and hydrological observations will be combined to provide a better understanding of rupture processes of large earthquakes.

The WFSD scientific goals have been and will be reached through various analysis of rock samples from the boreholes, online fluid geochemical monitoring, borehole geophysical logging, as well as direct stress and seismic observations, to better understand the following four aspects: 1) determination of the composition, texture and structure of the fault zones; 2) reconstruction of the physical and chemical properties of the fault zones, such as including fluid pressure, permeability, seismic velocities, electrical resistivity, density, porosity, etc.; 3) better understanding of the mechanism of the fault that ruptured during the Wenchuan earthquake; 4) long-term monitoring from instruments installed in the boreholes after drilling completion.

This paper reports preliminary data on the lithology, stratigraphy, fault-related rocks and structures of WFSD-1 drill cores, as well as the geometry of observed fault zones and Principal Slip Zone (PSZ) of the Wenchuan earthquake.

2. Tectonic setting

2.1. Longmenshan tectonics

The Longmenshan lies at the eastern margin of the Tibetan Plateau, west of the Sichuan Basin, and is marked by a steep topographic gradient and a high topographic relief of 3000–4500 m. The Longmenshan is the topographic boundary between eastern and western China, and is also the central segment of the NS-trending seismic belt in China, as well as one of the most active seismic zones (Deng et al., 1994). The Longmenshan fault zone is the easternmost thrust belt of the Songpan–Ganzi orogen (Xu et al., 1992) and is mainly composed of three thrust faults: the Wenchuan–Maoxian, Yingxiu–Beichuan and Anxian–Guanxian faults, from west to east, respectively (Fig. 1) (Li et al., 2006; Wang and Meng, 2008). The Longmenshan region can be divided into four parts from west to east: Paleozoic metamorphic terrain, Precambrian metamorphic complexes (represented by the Pengguan and Baoxing complexes), Triassic coal-bearing strata (such as the Xujiahe formation) and Jurassic foreland basin. Xu et al. (2007) suggested that an early Cretaceous ductile detachment belt developed along the Wenchuan-Maoxian fault (detachment along the eastern margin of the Tibetan Plateau), yielding the tectonic extrusion of the Pengguan and Baoxing complexes. As a strike–slip thrust fault zone, the Longmenshan fault zone is characterized by thrust-sinistral strike–slip motion from late Triassic to Paleogene (Li et al., 2006; Wang et al., 2001, 2008), and by thrust-dextral strike–slip motion since the Meso-Cenozoic (Densmore et al., 2007; Li et al., 2006; Wang et al., 2008). The Longmenshan fault zone has long been active and its currently active faults have developed along the previous faults since the late Triassic (Burchfiel et al., 1995; Deng et al., 1994; Densmore et al., 2007; Li et al., 2006; Wang and Meng, 2008; Z.Q. Xu et al., 2008; R.J. Zhou et al., 2006).

GPS measurements indicate a very slow deformation rate at a 10 yrs-scale with less than 2 mm/yr (Zhang et al., 2008), suggesting that the Longmenshan fault zone has been locked (Z.Q. Xu et al., 2008), with a rather long recurrence interval for Ms ≥7.0 earthquakes (~3000–6000 yrs, Li et al., 2008; Zhang et al., 2008). Indeed, no earthquake larger than Ms 7.0 has occurred along the Longmenshan fault zone. Only three Ms 6.0–6.5 earthquakes struck along its south-central segment, and further north, two events happened in the Minshan region, i.e. the 1933 Ms 7.5 Diexi earthquake and the 1975 Ms 7.2 Songpan earthquake (Tang and Han, 1993). This means that there was a relatively long quiet period before the Wenchuan earthquake struck, with energy accumulation increasing the possibility of large earthquake occurrence. According to modern morphological and ancient surface rupture characteristics, earthquakes > Ms 7.0 have not occurred along the Longmenshan fault zone, as surface rupture zone can usually only be produced by earthquakes larger than Ms 7.0 (Feng, 1997).

2.2. Co-seismic surface rupture zone of the Wenchuan earthquake

The Wenchuan event (Ms 8.0) produced surface ruptures along the NE-striking Yingxiu–Beichuan and Anxian–Guanxian faults simultaneously, with about 270 km-long and 80 km-long surface ruptures, respectively (Fig. 1b), and is characterized by almost simple thrust faulting coupled with dextral slip (Fu et al., 2011; Li et al., 2008; Liu et al., 2008; Z.Q. Xu et al., 2008; X.W. Xu et al., 2008). In addition, a 6 km-long, NW-striking rupture zone characterized by thrusts from SW to NE coupled with sinistral slip component occurred in the Xiaoyudong area, which connected the two rupture zones mentioned above (Li et al., 2008; Liu et al., 2008; Z.Q. Xu et al., 2008; X.W. Xu et al., 2008). The rupture zones usually develop following preexisting fault traces.

Detailed offsets analysis shows two peaks along the Yingxiu–Beichuan rupture zone (Li et al., 2008), with Qingping town (Mianzhu City) being the boundary. To the south, the maximum vertical displacement is 6–6.7 m in Shenxigou and Bajiaomiao villages (Hongkou county) (Fu et al., 2011; Li et al., 2008, 2009; Liu-Zeng et al., 2010; Xu et al., 2009) while at Beichuan, the maximum vertical offset is ~11–12 m at Shaba village (Qushan county) (Fu et al., 2009; Li et al., 2008, 2009; Liu et al., 2008; Ran et al., 2010). The two segments generally correspond with two rupture processes indicated by seismic wave inversion (Wang et al., 2008; Zhang et al., 2009): the south is a thrust with some dextral strike–slip motion, while the north is almost purely dextral strike–slip.

3. Drilling overview

The first hole of the Wenchuan earthquake Fault Scientific Drilling (WFSD-1) (N31.149°, E103.691°) is located in Bajiaomiao village, Hongkou county (Dujiangyan, Sichuan), on Pengguan complex rocks, which represent the hanging wall of the Yingxiu–Beichuan fault zone (Figs. 1 and 2). It is located 385 m west of the Wenchuan earthquake surface rupture (Fig. 2), in order to meet the Wenchuan earthquake fault zone at as shallow depth as possible and to study the characteristics of the fault zone and monitor the residual friction heat that has been produced during the earthquake and its aftershocks. For these reasons, WFSD-1 was designed to be an inclined hole (80°) in the NE134° direction, i.e. perpendicular to the surface rupture zone which is ~NE40°.

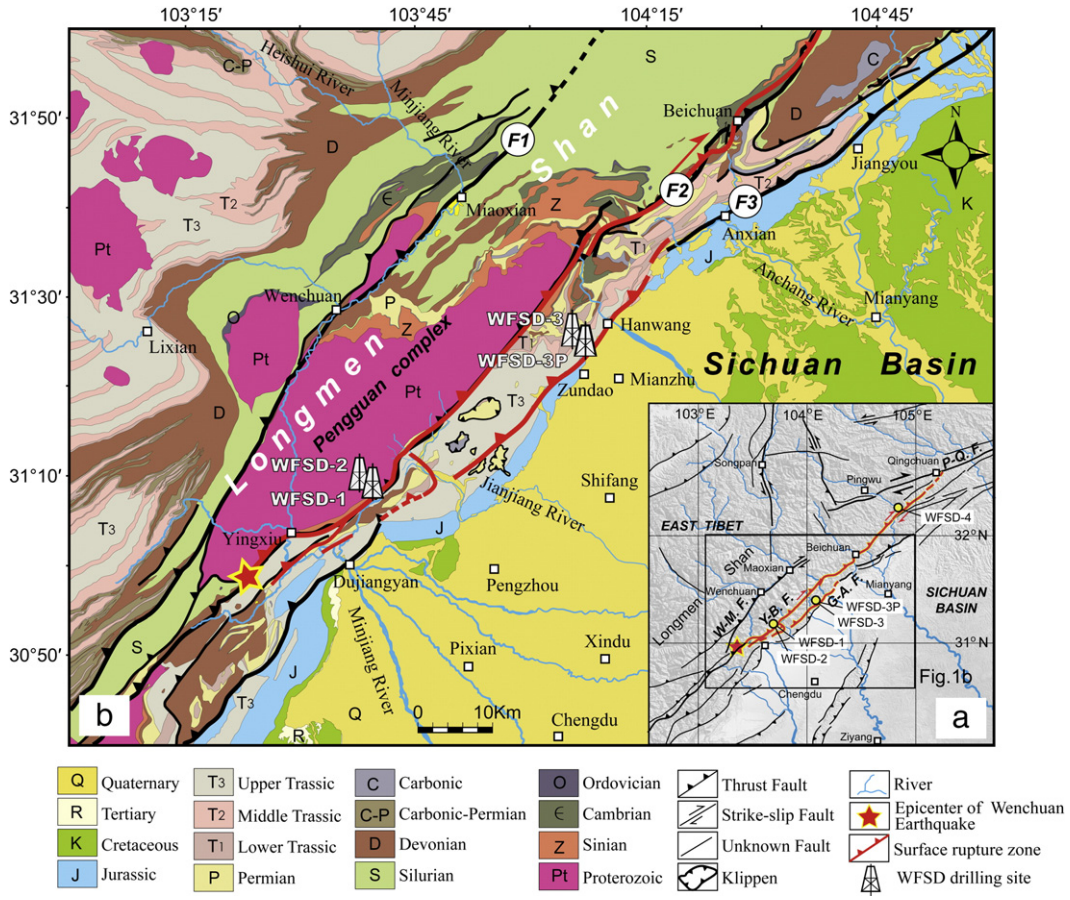

Fig. 1. Geological structures of the Longmenshan and its adjacent area and WFSD drilling sites location. F1: Wenchuan–Maoxian fault (W–M F.); F2: Yingxiu–Beichuan fault (Y–B F.); F3: Guanxian–Anxian fault (G–A F.); Pingwu–Qingchuan fault (P–Q F.).

Even though the drilling was initially planned for 3 to 4 months, it eventually took 8 months, with minor changes from the original plan (Fig. 3).

During the drilling process, many difficulties arose, such as crushed rocks, water gushing and borehole collapse, in addition to difficulties to retrieve the cores. For example, a fracture of the 127 mm-wide casing occurred at 167 m-depth, resulting in erroneous data (Fig. 3b). Therefore, we were forced to drill a second hole from 166.88 m-depth (Fig. 3a). At 585 m-depth, we reached the thick fault gouge with sandstone, siltstone and shale layers, which can expand and flow under in-situ stress, i.e. the borehole diameter dramatically shrank (Fig. 3c), leading to drilling tools jam and fractures three times in a row. We therefore had to sidetrack drill a third hole from 580 m-depth (Fig. 3a), after which the logging probe was blocked again at 705 m-depth. These difficulties lead to the low efficiency of the drilling process (Fig. 3b).

On March 2, 2009, the drilling tools were stuck at 590.76 m-depth, and broke while trying to pull them out. We tried several options but there were still more than 5 m-long drilling tools stuck in the hole. Finally, we had to cut the tools and lift out the fragments (Fig. 3b). On March 24, the 3.39 m-long drilling tools got stuck and broke again at 625.8 m-depth. On March 25, the same incident happened again (from 616.16 m-depth, with 2.14 m-long tools). But on July 12, WFSD-1 borehole reached a depth of 1201.15 m, with a total core length of 1368.29 m (total core recovery is 95.4%, Fig. 3g), with an average mechanical drilling speed of 1.07 m/h, average length for each run of 1.31 m, an end angle of the hole of 13.5° (Fig. 3e) and a hole azimuth of 168° (Fig. 3d). All cores were described immediately after retrieval in order to avoid the effects of disturbance, and described in details in the field laboratory.

4. Core description

At WFSD-1, above 285 m-depth, the core diameter is 76 mm-wide; from 285 to 810 m-depth, it is 67 mm-wide; and below 810 m-depth, it is 46 mm-wide. The cores consist of diorite and porphyrite, volcanic rocks, pyroclastics, sandstone (including coal-bearing sandstone), siltstone, shale, liquefied breccia (soft sediment deformation, Qiao et al., 2012) (Figs. 4 and 5), and a series of fault-related rocks (Figs. 6 and 7). The diorite, volcanic rocks and pyroclastics make most of the Neoproterozoic Pengguan complex which can be seen above 585.75 m-depth, i.e. the boundary zone (fault zone) of the Pengguan complex and Upper Triassic Xujiahe formation. Below 585.75 m-depth lies the Xujiahe formation which consists of sandstone, siltstone, shale and liquefied breccia (Figs. 4 and 5c–g). Fault-related rocks can be seen in both the Pengguan complex and Xujiahe formation.

4.1. Lithology and stratigraphy

4.1.1. Pengguan complex

Located in the central part of the Longmenshan, the Pengguan complex is lens-shaped in the Wenchuan-Maoxian and Yingxiu–Beichuan faults (Fig. 1), and constitutes most of the Longmenshan fault belt. To the north, the contact with sedimentary rocks is discordant while to the south, there is a contact between Paleozoic and Triassic strata (Fig. 1). The Pengguan complex mainly consists of biotite granite, plagiogranite, mylonite, granodiorite, tonalite, intermediate-acidic intrusive rocks similar to diorite, and some mafic–ultramafic intrusive rocks, volcanics, pyroclastic rocks and metamorphic rocks of green schist phases (Chengdu

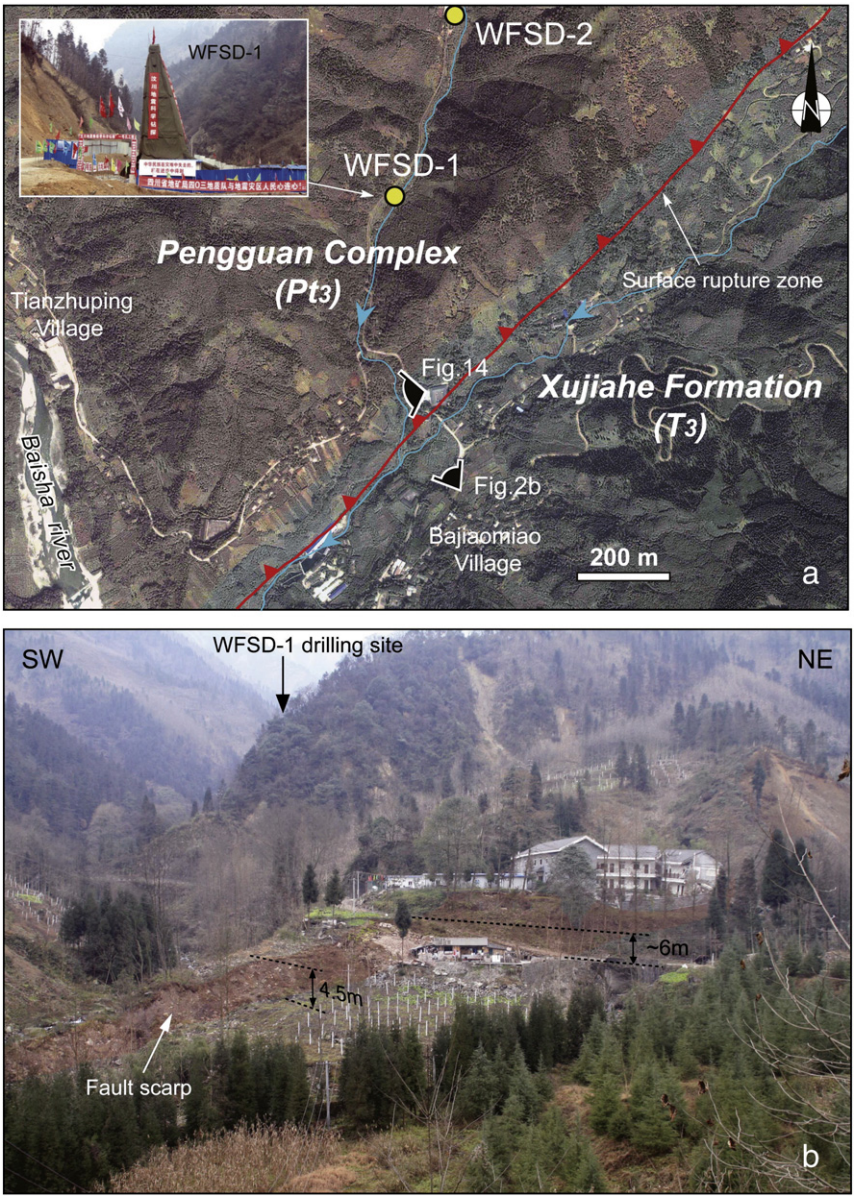

Fig. 2. (a) Satellite image (Google Earth) of WFSD-1 and 2, with co-seismic surface rupture zone striking N46°E (red line) and (b) the 4.5–6 m-high Wenchuan earthquake fault scarp, lying within the Upper Triassic sediments (Xujiahe formation, light blue in (a)). The light pink area represents the Neoproterozoic Pengguan complex.

Institute of Technology, 1996; Li et al., 2002; Ma et al., 1996; Sichuan Bureau of Geology, 1975). The zircon U–Pb age of the granite, diorite and gabbro is 859–699 Ma (Ma et al., 1996), and the SHRIMP age is 850–750 Ma (Yan et al., 2004), showing that the Pengguan complex is the result of Neoproterozoic magmatic activity. The western side of the Pengguan complex near Xuelongbao adak complex has a SHRIMP zircon U–Pb age of 748 ± 7 Ma (M.F. Zhou et al., 2006).

From 3 to 181.5 m-depth, WFSD-1 cores (Fig. 4) are pyroclastics, which mainly consist of celadon tuff. The main rock composition of cores from 181.5 to 291 m-depth are porphyrite and diorite, with three intervals of volcanic rocks: 189–196 m, 226–249 m, and 271–276 m. Pyroclastic and volcanic rocks are highly altered and often difficult to distinguish under naked eyes, therefore called "volcanics" in Fig. 4. From 291 to 575.6 m-depth are mainly volcanic rocks and pyroclastics, except three intervals of diorite and porphyrite, which are located at 362.7–394 m-depth, 494–512 m-depth and 545–555 m-depth. From 575.6 to 585.75 m-depth we find mostly cataclasite. The host rocks identification using thin sections will be described elsewhere.

4.1.2. Xujiahe formation

Non-metamorphosed upper Triassic series are located east of the Yingxiu–Beichuan fault (Fig. 1) and consist of the Maantang, Xiaotangzi and Xujiahe formations, with the latter being divided into six lithologic sections in the Longmenshan area (Chengdu Institute of Technology, 1996; Qiao et al., 2012; Sichuan Bureau of Geology, 1975). The first section is composed of marine sediment layers, such as quartz sandstone. The second section is mainly made of gray–light-gray sandstone, lithic sandstone fixed with siltstone and dark-gray mudstone, sandy mudstone and coal-lines. The third section consists of dark-gray mudstone, sandy mudstone, light-gray lithic sandstone, and inter-bedding of rich lithic sandstone and siltstone, with the middle and lower parts mixed with carbon shale and coal-lines. The fourth section consists of gray, fine to medium grain lithic sandstone, conglomerate with fragments of limestone and some sandstone, siltstone and inter-bedding of dark-gray mudstone and sandy mudstone layers fixed with coal-lines. The fifth section is mainly composed of dark-gray mudstone, sandy mudstone, gray fine grain lithic sandstone, rich-lithic sandstone, feldspathic litharenite, siltstone interbedded with plant fossils and

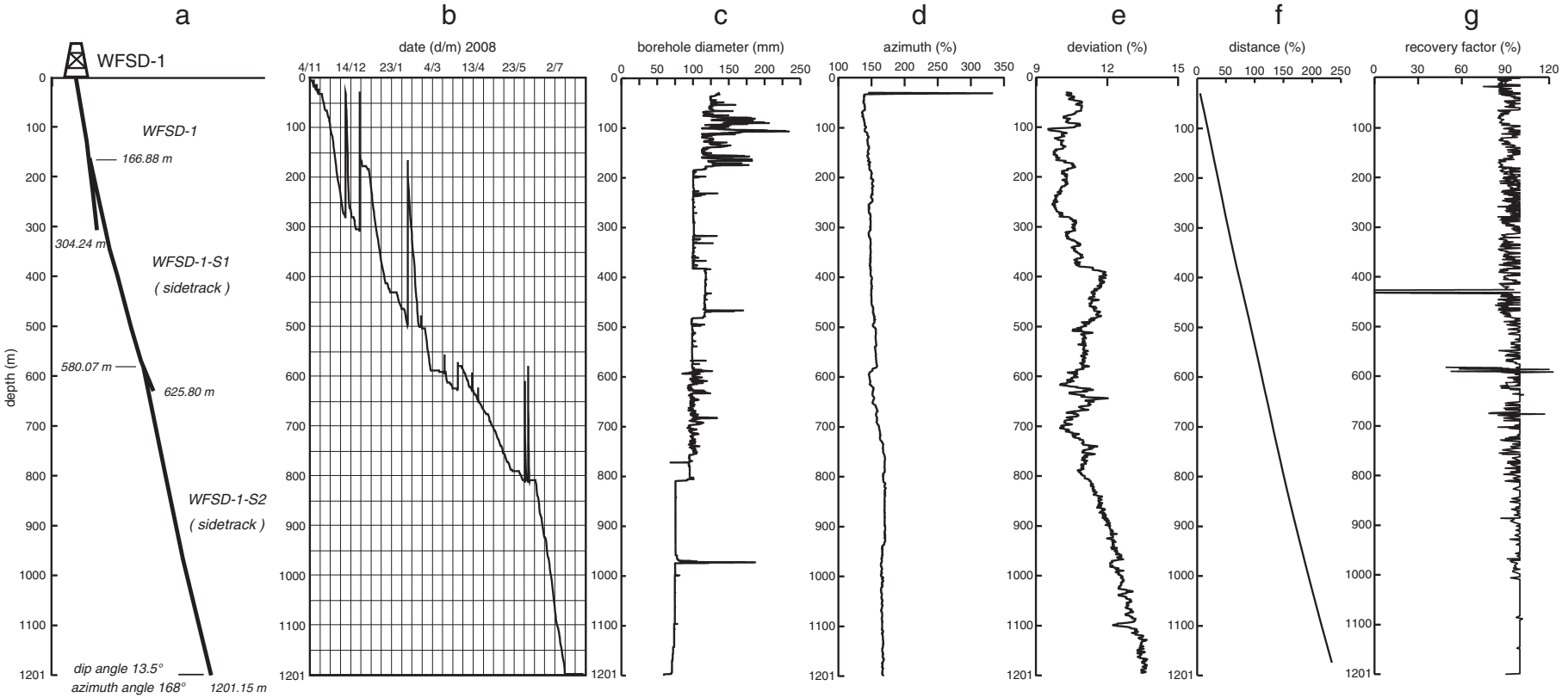

Fig. 3. WFSD-1 borehole. (a) hole sketch, the second hole from 166.88 m-depth and the third hole from 580 m-depth; (b) Problems occurred at depth of ~300, 500, 600 and 800 m, when starting logging and casing, and sidetrack-drilling at depth of ~166.88 and 580 m; (c) borehole diameters; (d) borehole inclination; (e) borehole dip angle; (f) drilling trace perpendicular to the surface rupture; (g) core recovery percentage, the cores were lost at about 430 m-depth.

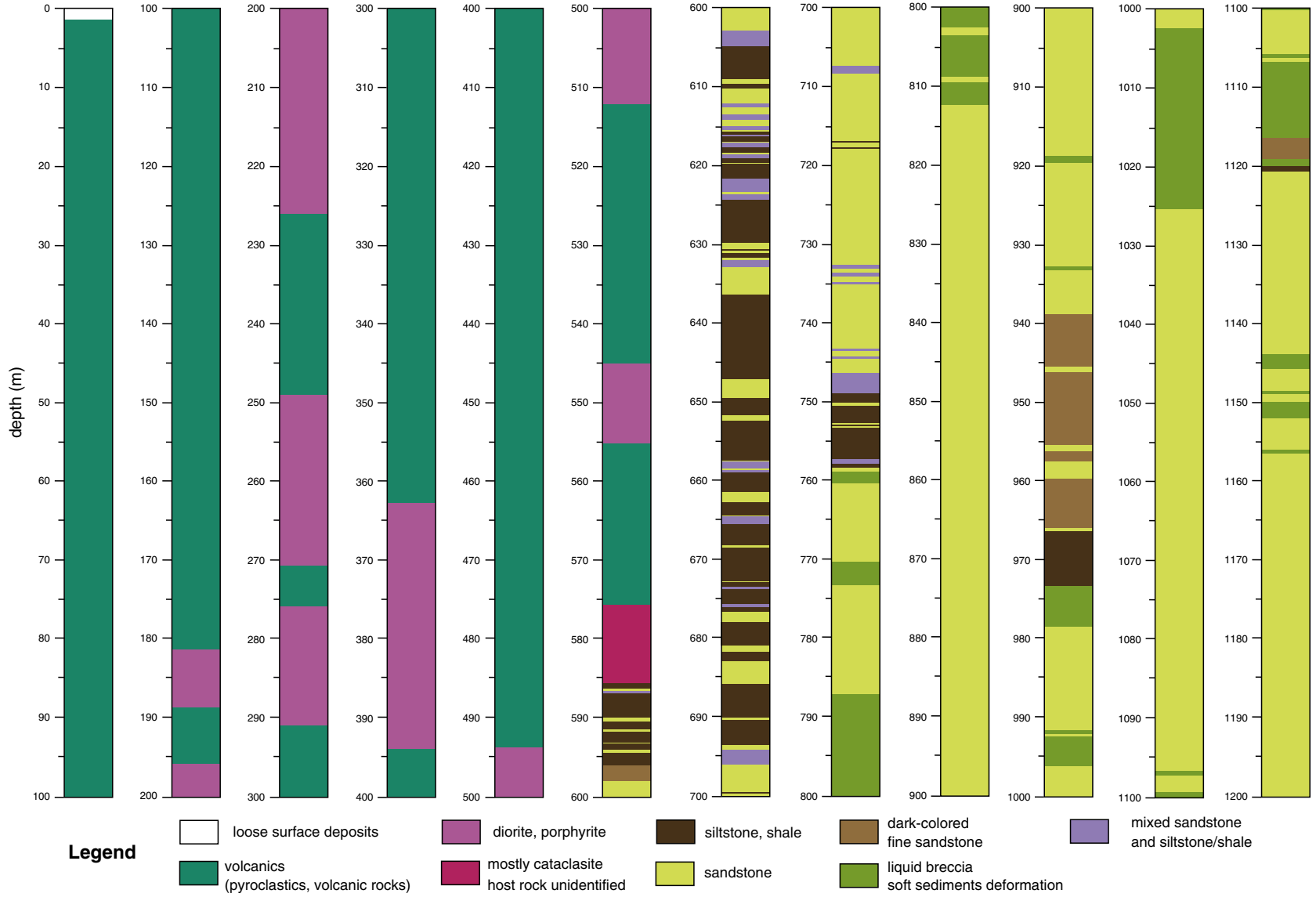

Fig. 4. Lithology chart of WFSD-1 cores (original rock), with depths being the borehole depths.

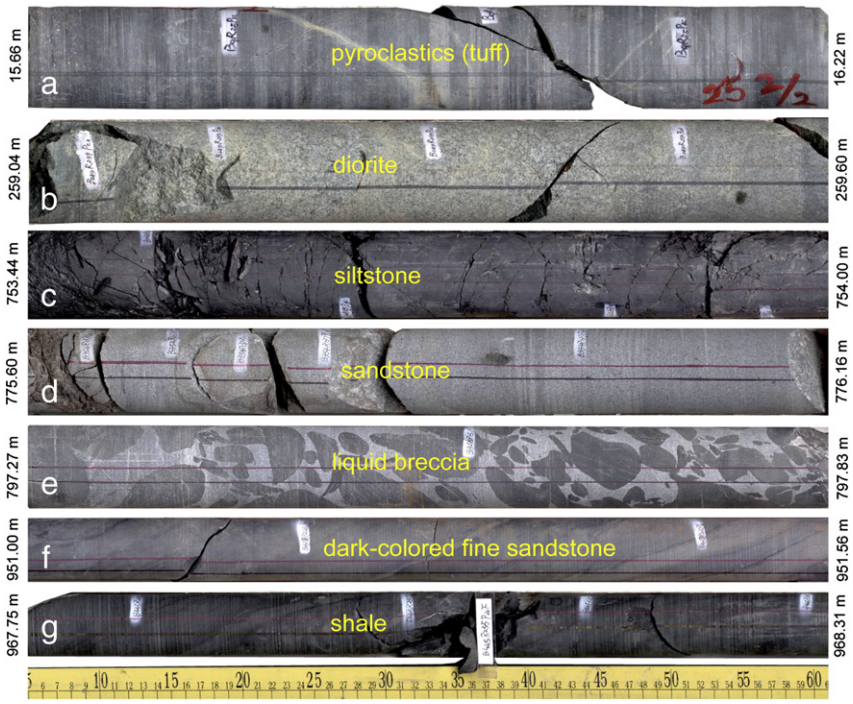

Fig. 5. Photos of WFSD-1 cores. Pyroclastics (tuff) (a) and diorite (b) in the Pengguan complex; siltstone fragment in the fault breccia zone (c), sandstone (d), liquid breccia (e), dark-colored fine sandstone (f) and shale (g) in the Xujiahe formation.

coal-lines. The sixth section is not present in the Longmenshan area. The WFSD-1 drilling site and its surrounding area are similar to the second and third sections of the Xujiahe formation.

In the WFSD-1 cores (Fig. 4), from 585.75 to 759 m-depth, the lithology of the cores are mainly gray sandstone, dark-gray siltstone, carbon shale and coal-lines, some parts are sandstone mixed with siltstone and shale. If rocks contain more than 2/3 of sandstone, they are described as sandstone in Fig. 4. Likewise, rocks shown as "siltstone/shale" contain more than 2/3 of siltstone and shale, and "mixed sandstone and siltstone/shale" consists of mixed sandstone and siltstone/shale each with less than 2/3. Below 759 m-depth are mainly gray sandstone, dark-colored fine sandstone and liquefied breccia (soft sediment deformation). The 585.75 to 759 m-depth core lithology corresponds to the third section of the Xujiahe formation, and the lithology below 759 m-depth corresponds to its second section. We observe that the order is identical to the Xujiahe formation in the WFSD-1 cores.

4.2. Fault-related rocks

The classification of the fault-related rocks in the WFSD-1 cores adopt the Sibson (1977) classification based on the structure (foliated versus random), lithification (incohesive versus cohesive) and fraction of visible clasts versus matrix where grains are invisible under naked eyes. We add foliated fault gouge and foliated cataclasite after Chester et al. (1985) since those fault rocks are fairly common. Predominant

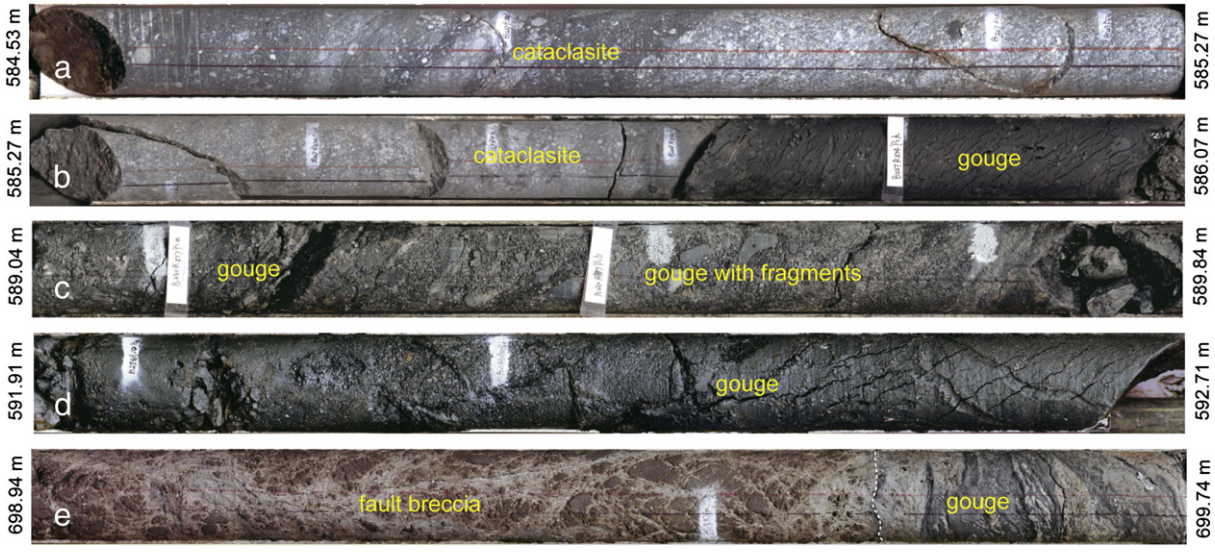

Fig. 6. Photos showing fault-related rocks in WFSD-1 cores. (a) Directional properties showed by different colors in cataclasite; (b), (c), (d) directional cracks are observed along the foliation in the black gouge; (e) sandstone fragments in fault breccia.

Fig. 7. Deformation structure characteristics of fault-related rocks in WFSD-1 cores. (a) Fault-related rocks at 232.50–233.33 m-depth in FZ233; (b) Steep striation in the fault plane which lies at the bottom of (a), indicating pure thrust component; (c) oblique thrust striation; (d, e, f) "Mirror structure"; (g) striation and steps in the fault plane.

fault rocks in WFSD-1 cores are fault gouge, fault breccia and cataclasite formed in the Pengguan complex and Xujiahe formation (Fig. 6), but we have yet to confirm the presence of pseudotachylite.

The fault gouge is an incohesive, often clay-rich, fine-to ultra-fine-grained rock with or without foliation and has less than 30% of visible fragments. In WFSD-1, gray to dark-gray and black gouges developed in different lithologic rocks (Fig. 6). Some gouges were soft with high water content when retrieved from the borehole, and dried after 1 day due to evaporation, and seasonal crack directions seem to be parallel to the fault slip zone (Fig. 6d). Some gouges were hard when retrieved from the drilling hole, i.e. formed at an early stage, while the soft gouges might have formed relatively recently. In all WFSD-1 cores, the thickness of the gouges vary from a few millimeters to a few meters (Fig. 8). More than 2, 3 and 2.5 m-thick gouges are present from 587.8 to 590.1 m, 605.7 to 608.7 m and 636.5 to 639.1 m-depth, respectively, representing the thickest gouge zones in all WFSD-1 cores (Fig. 8).

In WFSD-1 cores, cataclasites mostly with dark to light-gray color are present in the Pengguan massif and are abundant near the boundary with a side incohesive fault zone in the Triassic sedimentary rocks (Figs. 6a, b and 8). Fragments of cataclasites are also contained in the wide fault zone from 586 to 759 m-depth, consisting of fault breccia and gouge (Fig. 8).

Fault breccias in WFSD-1 cores are readily distinguished by the visible clasts of >30 volume % in fine-grained matrix (Fig. 6e) and are associated commonly with fault gouges in the major fault zone. Lithologic profile of WFSD-1 cores (Fig. 4) indicates that fault breccia and gouge consist mostly of Triassic sedimentary rocks although some clasts of Pengguan massif are mixed in near the massif boundary.

Pseudotachylyte is a dark, extremely fine-grained, often glassy rock forming veins or dykes, typically associated with shear zones or faults. It is interpreted as large fossil remnants from paleoseismic events (Lin et al., 2001; Magloughlin and Spray, 1992; Sibson, 1975; Theunissen et al., 2002). In TCDP Hole-A, pseudotachylyte could only be observed under a Transmission Electron Microscope (TEM) from a depth of 1111.29 m of the PSZ during the 1999 Chi-Chi earthquake (Mw 7.6) (Kuo et al., 2009). We have not confirmed the presence of pseudotachylyte in the WFSD-1 cores yet.

5. Deformation structure

5.1. General description

Most of the WFSD-1 cores are typically broken, containing many calcite veins, fault breccias, cataclasites and fault gouge with different orientations. There are also various kinds of slickenside in some fault planes indicating different tectonic features (Fig. 7), and many polished gouge fault surfaces ("mirror structure") (Fig. 7d, e, f). Calcite veins formed in the fault zones and along fractures, and steps can be seen occasionally on fault planes displaced along the veins (Fig. 7g).

Fractures occur in the entire WFSD-1 cores with similar densities but different dip directions (Fig. 9). Above 600 m-depth, fractures bearing dip directions of N170° to N270° and angles of 40°–70° are dominant, and some have dips of N270° to N360°. Although void of logging data, the fracture characteristics between 596 and 780 m-depth might be similar to the 680–830 m interval according to the fractures density distribution pattern (Fig. 9b). The fractures from the cores below 780 m-depth have dip directions (N40°–N100°) and dip angles (60°–80°) different from the upper interval (Fig. 9c, d). From the surface to ~600 m-depth, the fault planes have dip directions of N220°–N360° (Fig. 9e) and dip angles of 50°–80° (but mainly 60°–75°, Fig. 9f). The planes at 972 and 1133 m-depth have dip directions of N30° to N120° and dip angles of 40°–80° (Fig. 9e, f). Even though no logging data are available from 596 to 780 m-depth, cores observation shows that some fault zones are similar to the fault zone at 590 m-depth, even though they dip at N220°–N360° with angles of 60°–75°.

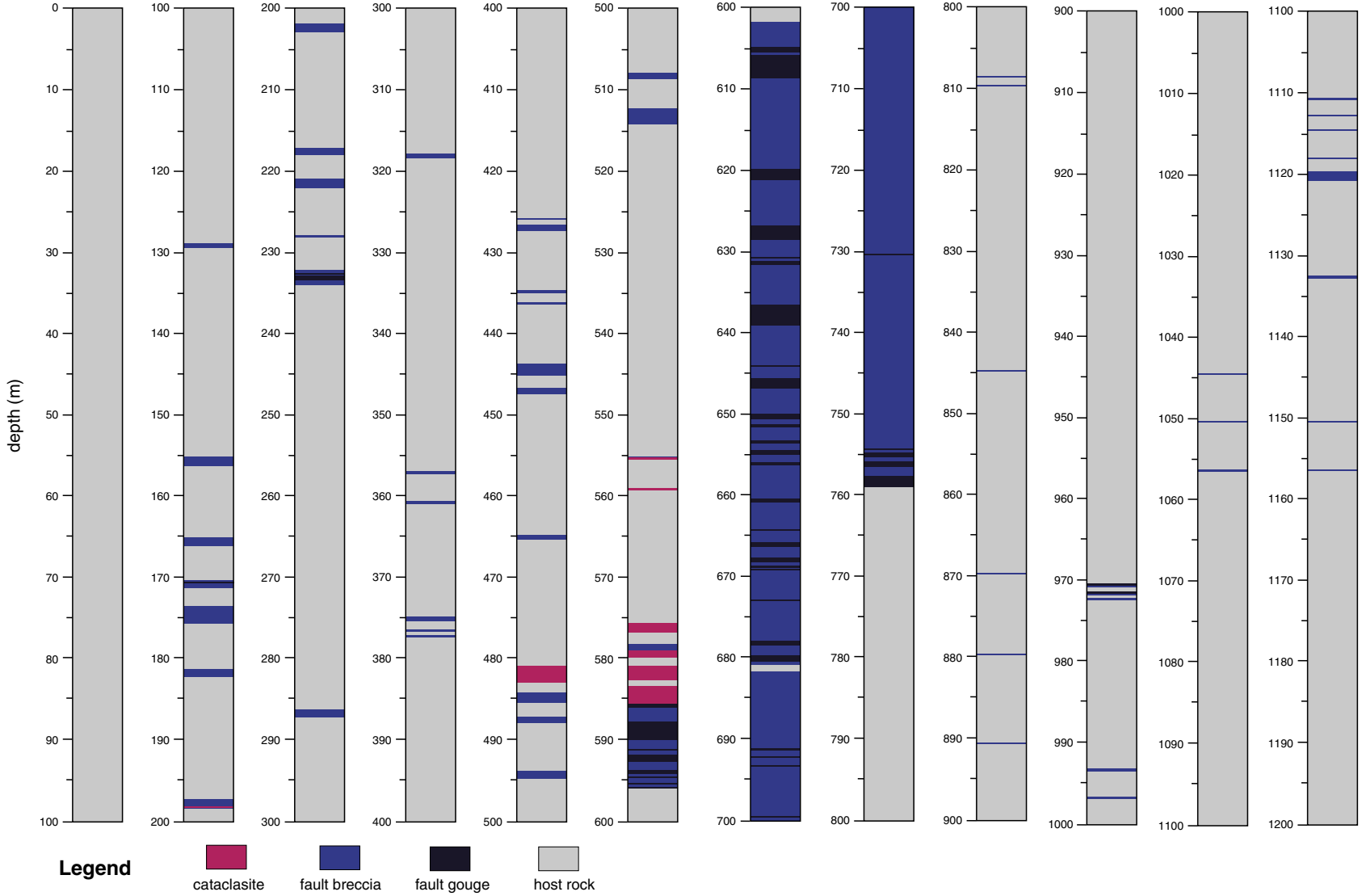

Fig. 8. Distribution of fault rocks along WFSD-1 cores. A large zone of the fault rocks continuous distribution at depths between 575.7 and 759 m, some host rocks belong to the clasts in the fault breccia zone, such as the rocks at 595.48–602.65 m-depth.

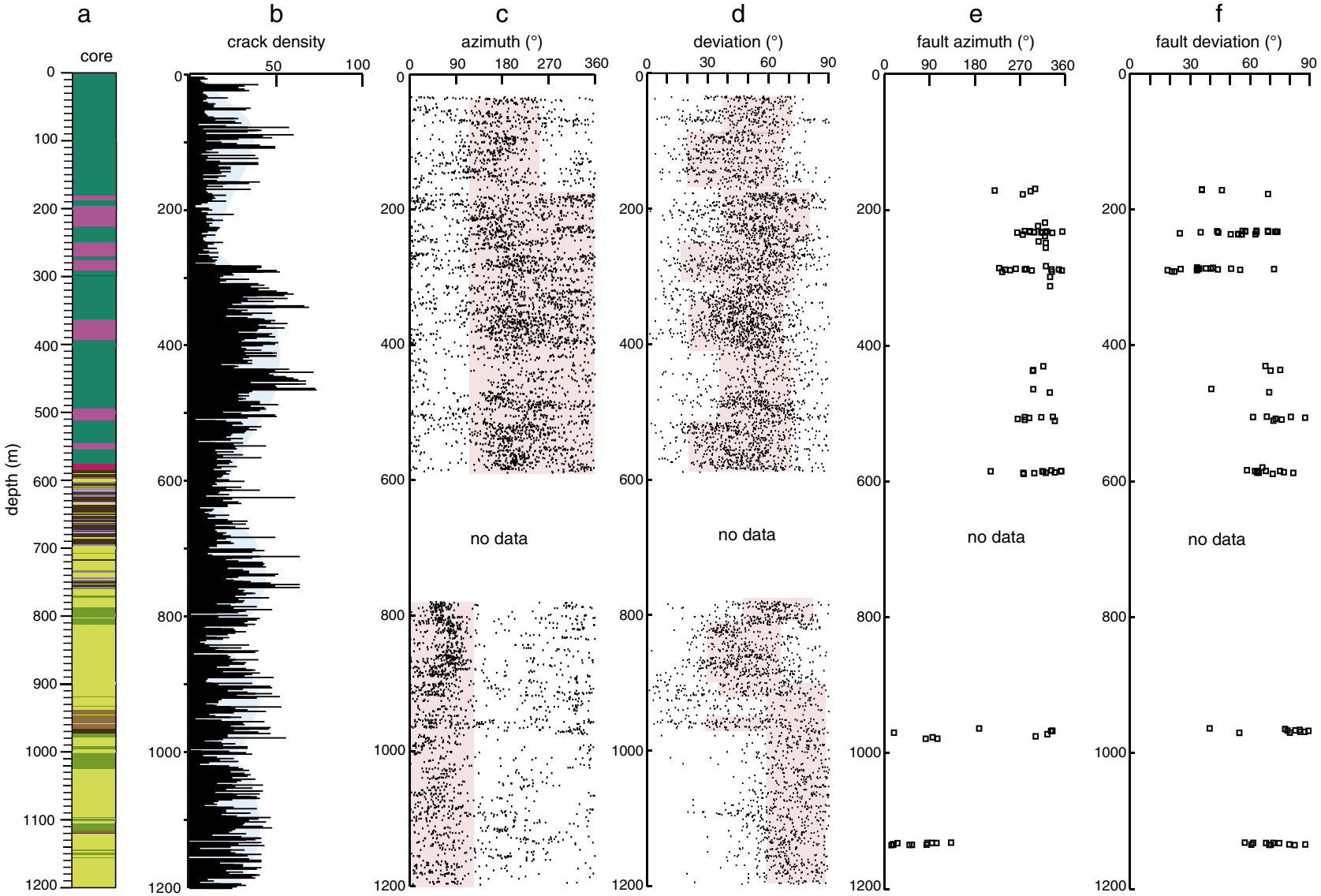

Fig. 9. Distribution of deformation structure in WFSD-1 cores. (a) Lithologic chart; (b) crack density chart; (c) structure tendency; (d) structure dip angle; (e) fault zones azimuth; (f) dip angle of fault zones.

Based on the geophysical logs data and the structural characteristics of the cores, we determined the major and subsidiary faults, which showed distinct zonation including cataclasite, breccia and gouge. Indeed, the damage zones contain many fractures network, making it difficult to determine the fault location. However, most of the contact boundaries between the gouge zones and the adjacent layers are very distinct and intact (Fig. 10), and this is favorable to get clear sonic images to distinguish contact planes. Fault gouges are the major slip zone which could represent the fault location. Thus, we used the gouge zone locations to represent those of the faults.

Dipole Sonic Imager (DSI) logs in the WFSD-1 hole was used to record high-resolution borehole sonic images in order to identify bedding planes, contact boundary between different rocks, fractures and shear zones. These measurements are used in drilling projects to obtain the sub-surface structures. Using the dip-log data, we determined accurate angles between the fault slip planes and the borehole walls containing their spatial parameters (Fig. 10), and the professional software for the dip-log synchronously yielded the occurrences. The results being most accurate when drilling vertically, the oblique WFSD-1 hole forced us to correct for the hole azimuth to obtain the actual fault occurrences (Fig. 9e, f).

5.2. Fault zones

The WFSD-1 cores contain many fault zones/cores. To determine their activity, we counted the fractures (fault cores) every 50 cm to obtain the fault factor. To highlight the fault rocks and calculate the fault (core) density, we give the weighted value to fault breccias, cataclasite and gouge at 10, 5 and 1 cm, respectively (Fig. 11).

The calculation formula is: fault density = (fault factor) + [(fault breccia length)] × 6/10 × [(weighted value for fault breccia)] + [(cataclasite length) × 7/5 × (weighted value for cataclasite)] + [(gouge length) × 8 × (weighted value)], where fault factor varies from 0 (without fracture) to 5 (partially breccia); fault breccia length is the length of breccia every 50 cm core; weighted value for fault breccia is 1 (length <10 cm), 2 (length 10–30 cm) or 4 (length >30 cm); cataclasite length is the length of cataclasite every 50 cm core; weighted value for cataclasite is 1 (length <5 cm), 2 (5 cm<length ≤20 cm), 4 (20 cm<length ≤30 cm) or 8 (30 cm<length ≤50 cm); gouge length is the length of gouge every 50 cm core; weighted value for gouge is 1 (length <1 cm), 2 (1 cm<length ≤10 cm), 4 (10 cm<length ≤20 cm), 8 (20 cm<length ≤30 cm), 16 (30 cm<length ≤40 cm) or 32 (40 cm<length ≤50 cm). This method of calculation for the WFSD-1 cores allowed us to obtain the distribution of the fault density along the core (Fig. 11).

Based on the fault rock distribution features (Fig. 8) and fault density (Fig. 11) of WFSD-1 cores, a total of 12 major fault cores (zones) have been recognized from 30 to 1201 m-depth and named after their depth as FZ233, FZ590, FZ608, FZ621, FZ628, FZ639, FZ646, FZ655, FZ669, FZ678, FZ759 and FZ970. The fault cores (zones) bear different widths from 1.52 to 14.28 m and different gouge thicknesses ranging from 0.72 to 3.79 m (Table 1). The thickest gouges are those from FZ590 (3.79 m), FZ608 (3.62 m), FZ628 (2.9 m) and FZ639 (2.91 m). The fault zones have cumulative thick gouge layers composed of many fault cores with thin gouge layers (such as FZ590 and FZ608). The real gouge width and thickness should be multiplied by sin θ (where θ is the dip angle). In combination with the fault density profile (Fig. 11), three fault cores (zones) (FZ233, FZ590 and FZ759) with a higher density might suggest an intense and long-term activation. The three fault cores (zones) are located in the Pengguan complex (FZ233), the Late Triassic Xujiahe formation (FZ759) and the boundary zone (FZ590).

5.2.1. FZ233

The FZ233 fault core (zone) ranges from 232.2 to 233.9 m-depth in volcanic rocks with significant fracture deformation (Table 1, Figs. 4, 8 and 11). FZ233 is composed, from top to bottom (Fig. 12), of fault breccia (~36 cm), dark-gray gouge with fragments (~13 cm), fault breccia (~10 cm), dark-gray gouge with fragments (~34 cm), gray gouge (~25 cm), calcite vein (~10 cm) and fault breccia (~44 cm) (Figs. 8 and 12). According to the logging data, the gouge layers bear dip directions of N290°, and a dip angle of 74°. The fault zone is a pure thrust as indicated by the slickenside in the third gouge layer that bears the same dip direction as the fault plane (Fig. 9).

5.2.2. FZ590

FZ590 fault core (zone) ranges from 575.7 to 595.5 m-depth (Table 1, Figs. 8 and 11). FZ590 is located between the Neoproterozoic Pengguan

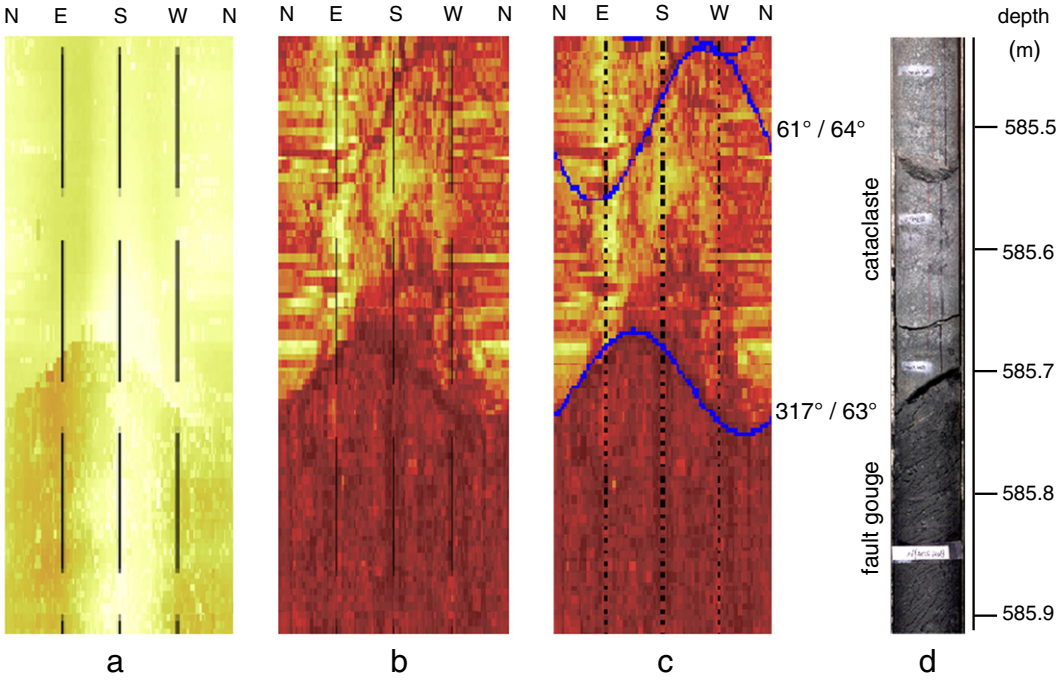

Fig. 10. Dipole Sonic Imager (DSI) logging of boundary between cataclasite and fault gouge zones in WFSD-1 cores. (a–c) Dipole sonic images, and (d) core from ~585.4 to 585.9 m-depth.

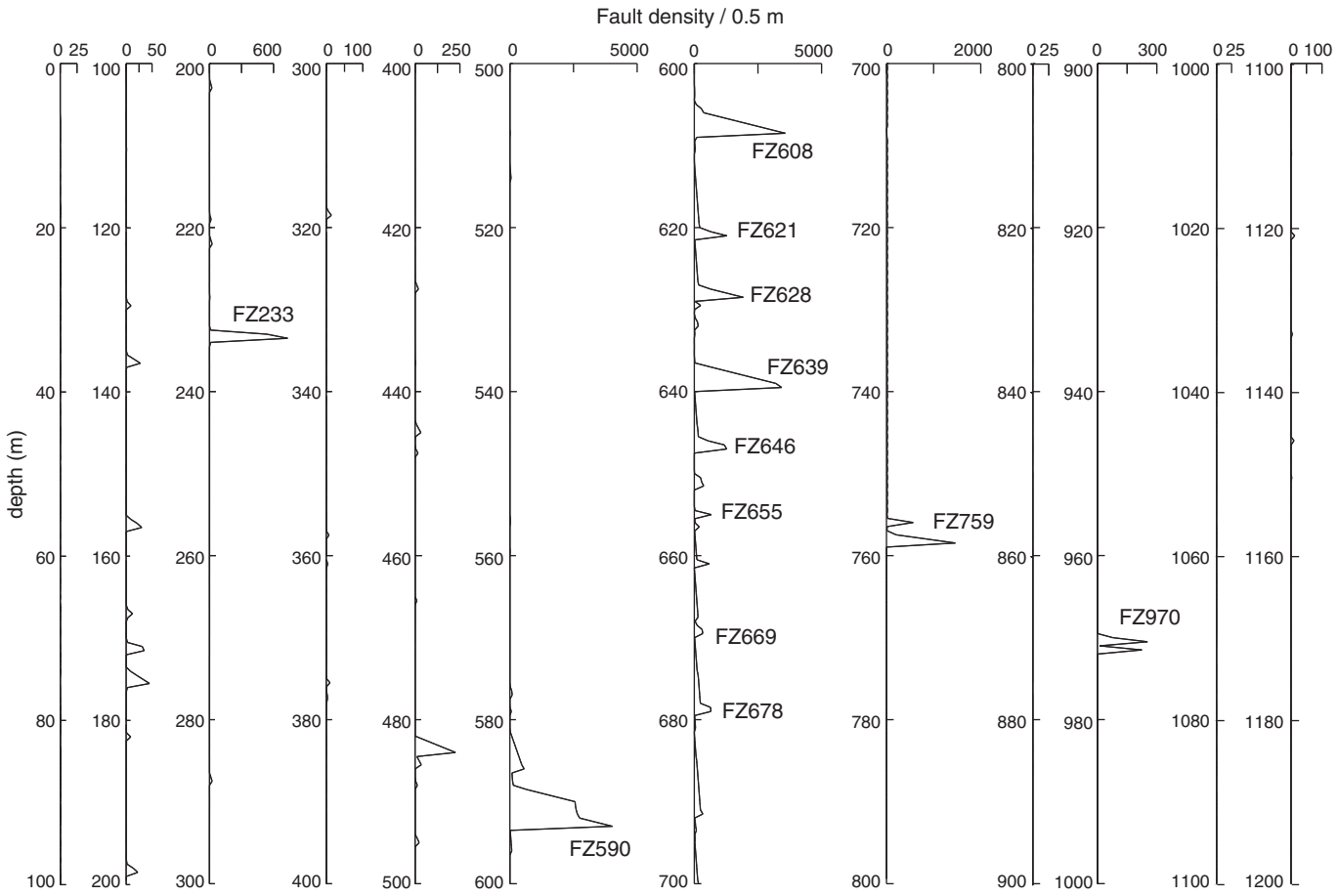

Fig. 11. Distribution of fault density profile of WFSD-1 cores. There are many fault zones/cores in the WFSD-1 cores. To determine their activity, different peak represent different fault (core) density. For specific calculation see the text.

complex and the late Triassic Xujiahe sedimentary rocks. From top to bottom (Fig. 13), FZ590 is composed of cataclasite (~118 cm), black gouge (~54 cm), fault breccia (~210 cm), black-dark-gray fragment-bearing gouge (~50 cm), black gouge (~94 cm) with ~8 cm black fresh gouge, fault breccia (~63 cm), black gouge (~30 cm), fault breccias (~10 cm), black gouge (~10 cm), fault breccia (~15 cm), dark gray-black gouge with calcite vein (~22 cm), fault breccia (~38 cm), dark gray-black gouge (~106 cm), fault breccia (~23 cm), dark-gray gouge (~13 cm), fault breccia (~207 cm) and dark-gray siltstone (~35 cm). The total thickness of the gouge is about 3.79 m. Black fresh gouge (~8 cm) is observed between 589.16 and 589.27 m-depth. The gouges were mostly soft with a high water content after being retrieved from the borehole, but many cracks formed parallel to the fault plane due to water evaporation when dry.

Logging data show that above 585.5 m-depth, the direction of the gouge boundary is N317° and the dip angle is 64°. There are 29 cracks and broken strips extracted from 585.4 to 594 m-depth, in which 19 strips have similar characteristics, with an average trend of N305° and average dip angle of 71°. This may represent the overall FZ590 characteristics.

5.2.3. FZ759

FZ759 fault core (zone) ranges from 753.13 to 759 m-depth (Table 1, Figs. 8 and 11), is composed of gray siltstone and shale (Fig. 4), and

Table 1
Characteristics of the major fault zones/cores in the WFSD-1 cores.

Fault zone		Top depth (m)	Bottom depth (m)	Total width (m)	Gouge width (m)	Gouge color	Water content	Hanging wall lithology	Footwall lithology
FZ233		232.2	233.9	1.7	0.72	gray	low	volcanics	volcanics
Yingxiu-	FZ590	575.7	595.5	19.8	3.79	black	high	volcanics	sandstone
Beichuan	FZ608	602.65	610.8	8.12	3.62	black	low	sandstone	sandstone
fault zone	FZ621	611.4	621.1	9.7	1.24	black	high	sandstone	pelite
	FZ628	621.1	634.2	13.12	2.9	black	high	pelite	sandstone
	FZ639	635.63	639.5	3.84	2.91	black	low	sandstone	sandstone
	FZ646	639.47	647.1	7.66	1.31	black	high	sandstone	sandstone
	FZ655	649.64	656.3	6.66	1.95	black	high	sandstone	pelite
	FZ669	656.3	669.1	12.8	1.31	black	high	pelite	pelite
	FZ678	669.1	680.9	11.83	0.85	black	high	pelite	pelite
	FZ759	753.13	759	5.9	1.94	black	high	pelite	sandstone
FZ970		970.26	971.78	1.52	0.86	black	high	sandstone	sandstone

Note: The gouge width is the cumulative width of all gouges present in the fault zone.

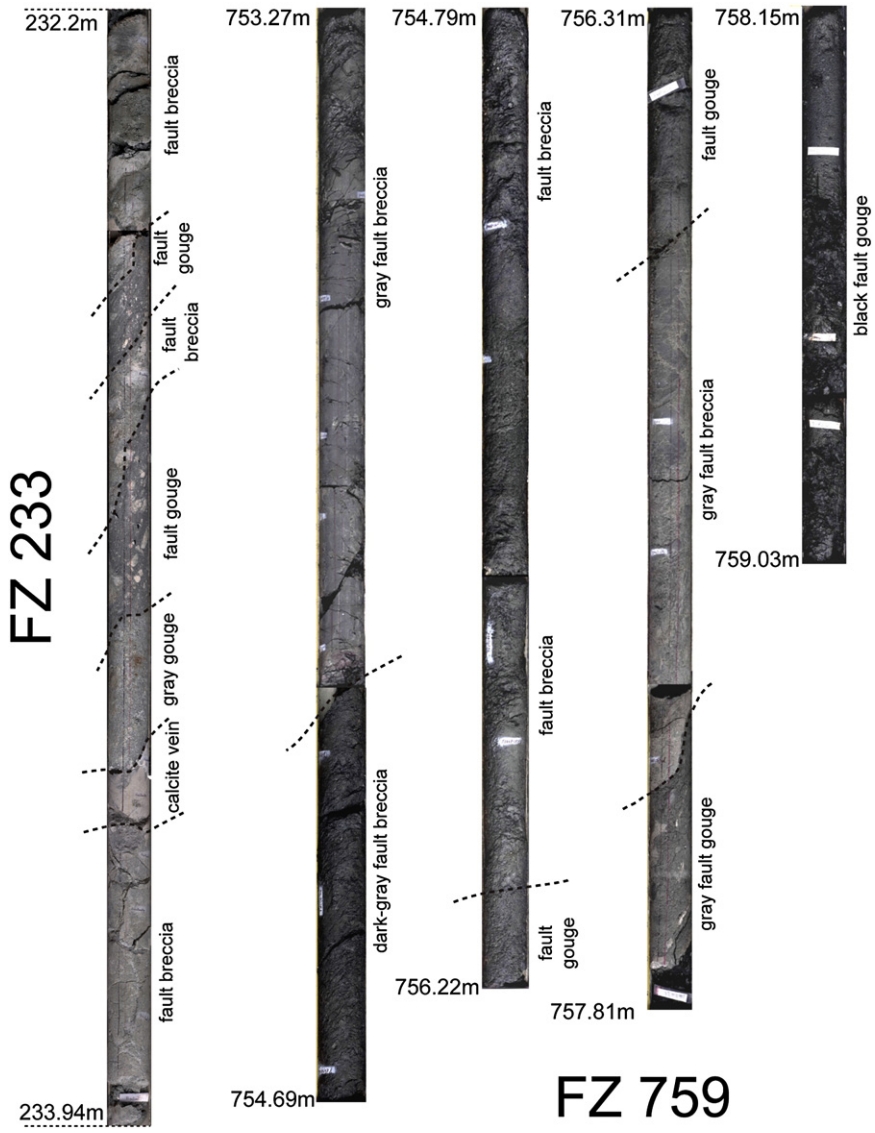

Fig. 12. FZ233 and FZ759 core photos with descriptive comments.

clearly belongs to the late Triassic Xujiahe formation. FZ759 from top to bottom (Fig. 12) consists of gray fault breccia (~95 cm), dark-gray fault breccia (~182 cm), fault gouge (~48 cm), gray fault breccia (~75 cm), gray fault gouge (~25 cm) and black fault gouge (~88 cm).

The intense core fractures may have similar characteristics as the gouges. Rupture planes are similar below 780 m-depth with directions of N40°–N100° (Fig. 9d) and dip angles of 60°–80° (Fig. 9e), which is in contrast with FZ590.

6. Discussion

6.1. Structure and width of the Yingxiu–Beichuan fault zone

It is generally acknowledged that there are two kinds of typical fault zone structures (Faulkner et al., 2010): (a) a single high-strain core surrounded by a fractured damage zone (Chester and Logan, 1986) and (b) multiple cores model, where many strands of high-strain material enclose lenses of fractured protolith (Faulkner and Rutter, 2003). The fault core generally consists of gouge, cataclasite or ultracataclasite (or a combination of these), and the damage zone generally consists of fractures over a wide range of length scales and subsidiary faults.

6.1.1. WFSD-1 cores

From our observation from the WFSD-1 cores (Fig. 8), the section from 575.7 to 585.75 m-depth is mainly composed of cataclasite, that from 585.75 to 759 m-depth is composed of a continuous fault zone with fault gouges of different scales, and fault breccia. Therefore, we confirm that the above two sections represent a large-scale fault zone. In addition, the 585.75 m-depth layer represents the boundary between the Neoproterozoic Pengguan complex and Late Triassic Xujiahe formation (Fig. 4), i.e. the Yingxiu–Beichuan fault zone, with a thickness of at least ~183 m (apparent thickness in cores along inclined drilling hole). The large fault zone is composed of many subsidiary fault zones (damage zone), and most of the subsidiary fault zones contain fault gouge, cataclasite, fault breccia and the host-rock with fractures. The fault gouge is located at the center of each fault core (zone). Both the WFSD-1 cores profile (Fig. 8) and a single fault core (e.g. FZ590, FZ608–FZ759) contain fault zone gouges, indicating a multiple cores model for the Yingxiu–Beichuan fault (Fig. 11). The multiple cores structure of the fault zone in the WFSD-1 cores is consistent with what was observed at the outcrop (Wang et al., 2010), i.e. that the fault zones in the cores have been foliated, and the gouge width ranges from several millimeters to a few meters, which is also consistent with the outcrop's study (Togo et al., 2011). Many fragments of cataclasite are contained in fault breccia in FZ590.

Fig. 13. FZ590 core photos with descriptive comments.

According to the logging data (Fig. 9) and continuous core analysis, FZ608, FZ621, FZ628–FZ678 and FZ759 have similar characteristics as FZ590, with an average orientation of N305° and an average dip angle of ~68°. These fault cores can be classified into one large fault zone. We therefore conclude that the dip angle of the Yingxiu–Beichuan fault zone is about ~68° at a depth of 759 m, and the fault zone is ~100 m-wide (with a core thickness of ~183 m, an average angle of ~11° along the inclined drilling hole). In contrast, FZ970, located in the footwall of the former group, is oriented ENE from N40° to N100°, with a dip-angle of 60° to 80°. Thus, since the latter does not constitute a back-thrust of the former group, it must be a different fault system.

6.1.2. Outcrop

In the Bajiaomiao outcrop of the Yingxiu–Beichuan fault zone (Fig. 14) (eastern tributary of the Baisha River, Fig. 2), the southern part is mainly composed of fault breccia and fault gouge (Fig. 14a, b, c, d) in the Xujiahe formation, and the northern part consists of cataclasite (Fig. 14a, e) in the Pengguan massif. The total length of the fault zone exposure along the tributary is approximately 200 m. The boundary between the Pengguan massif and Xujiahe formation is partly debris-covered (thick dashed line in Fig. 14a). The main fault zone, including a ~100 m-thick cataclasite discontinuous distribution zone and many fault gouges of a few millimeters to several meters long, is visible at the outcrops (Togo et al., 2011; Wang et al., 2010). The fault breccia and fault gouges are similar to our cores, while a ~100 m cataclasite discontinuous distribution zone is not observed. Fragment of cataclasite is contained in fault breccia as reported in Togo et al. (2011). Fault zones at outcrops are very similar to the fault zones seen in the cores, both in terms of width and fault rock types.

Along the outcrop, the Yingxiu–Beichuan fault is generally ~200 m-wide, striking N35°–46°E, dipping to the NW. The northern cataclasite and the southern fault breccias + fault gouge are ~100 m-wide. The black gouge is mainly visible near the cataclasite to the north (~4–6 m thick containing fault breccias) (Fig. 14d), and near the bottom of the fault zone (Fig. 14b). The co-seismic slip plane (strike of N46°E and dip of 75°NW) is at or near the bottom of the fault gouge zone (Fig. 14b), showing the asymmetry of the hanging wall, which is the fractured zone of the fault gouge and fault breccia zones, similar to the Nojima fault, whose fractured zone is confined in the hanging wall (Lin et al., 2007). The Yingxiu–Beichuan fault zone dips at about 75°, and is ~190 m-wide at the outcrop. If this asymmetry continues from the surface to depth through the whole fault zone, then the co-seismic slip plane of the Wenchuan earthquake should also occur at the bottom of the Yingxiu–Beichuan fault in the WFSD-1 core, i.e., in the black gouge layer at about 759 m-depth (FZ759 in Figs. 8, 11 and 12).

The geological evidence obtained from the outcrops and the WFSD-1 cores show different widths for the Yingxiu–Beichuan fault zone, ~190 and ~100 m, respectively. Therefore, the estimated fault plane dip angles are ~75°, 73° to 68° from the outcrop to ~760 m-depth (thick red dashed line FA in Fig. 17). The Yingxiu–Beichuan fault zone above ~760 m-depth is a fairly high-angle thrust fault.

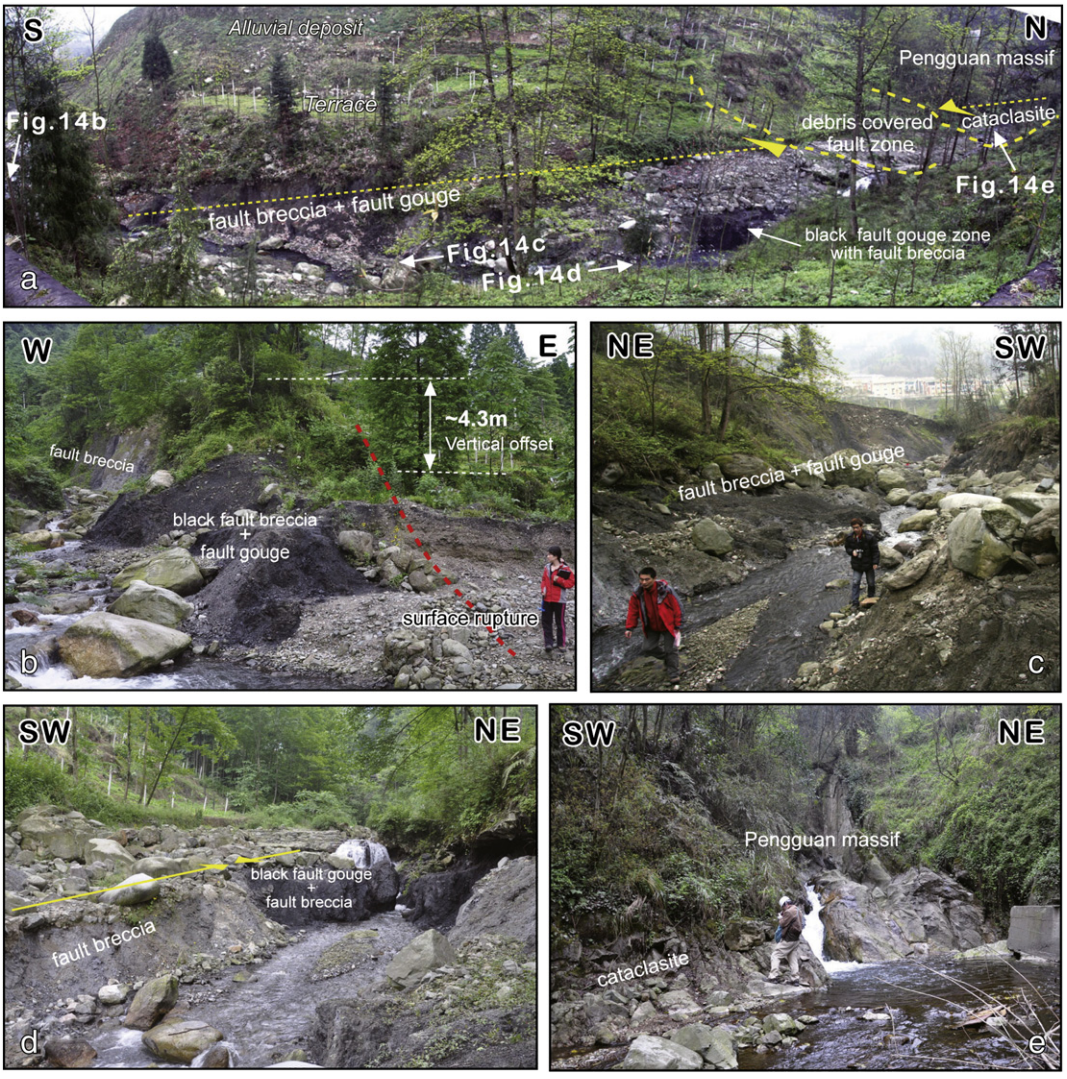

Fig. 14. Photos of outcrops of Yingxiu–Beichuan fault zone at Bajiaomiao village taken in March 2012. Location shown in Fig. 2. (a) Panoramic photo of the fault zone. Black fault zones (black fault gouges and/or black fault breccias) distribution at the bottom (b) and top (a, d) of the Xujiahe formation. Gray fault breccia and fault gouge zone (c) distribution between them, and (e) Pengguan massif (the cataclasite zone) in the northern outcrop. The red dashed line represents the co-seismic surface rupture zone of the Wenchuan earthquake (b).

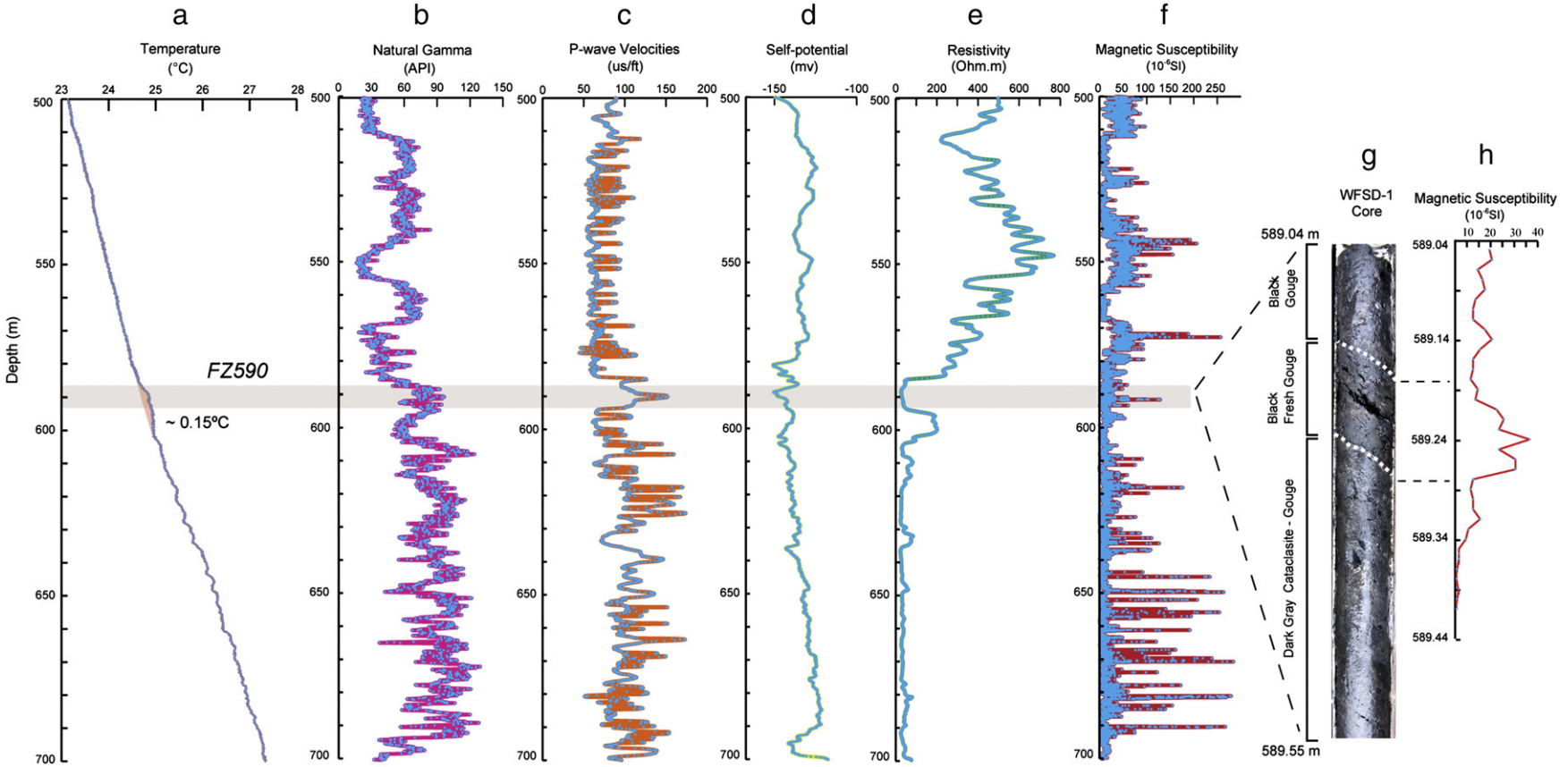

Fig. 15. Logging and core data of the main fault zone at 500–700 m-depth. All anomalies appear at 590 m-depth. (a) Borehole logging temperature curve, with ~0.15 °C anomaly peak, probably reflecting the residual heat which was produced by friction during the Wenchuan earthquake; (g) The Wenchuan earthquake Principal Slip Zone (PSZ) seems to be located where the freshest black gouge is.

6.2. The Principal Slip Zone (PSZ) of the Wenchuan earthquake

In order to locate the PSZ of the Wenchuan earthquake, we need to study the fracture mechanism, physical and chemical changes of the rocks, and analyze the long-term monitoring after the earthquake, i.e. temperature, fluid and stress field in the borehole after completing the drilling. There are at least 12 major fault cores (zones) in the WFSD-1 cores, each one with many gouge layers. Therefore, we are interested in determining which fault core (zone) was formed by the Wenchuan earthquake, and which layer of gouge represents its PSZ. A ~270 km-long surface rupture was identified along the Yingxiu–Beichuan fault zone, with the southern Yingxiu fault representing the boundary between the Neoproterozoic Pengguan complex and the Late Triassic Xujiahe formation sedimentary rocks.

According to the fault rocks distribution in WFSD-1 cores (Fig. 8), the gouges mainly occur at the top and bottom of fault zones, which is slightly similar to what we observe at the outcrop. If this is real, the PSZ of the Wenchuan earthquake might lie in FZ759 (FA showed in thick red dashed line in Fig. 17). However, after detailed observation of the fault gouge in the core, the fresh gouge seems to be present in FZ590, not FZ759. In addition, no anomaly in other logging data or temperature measurement data are observed in FZ759. We therefore conclude that FZ590 is the corresponding boundary that most likely represents the Wenchuan earthquake fault zone also due to the presence of the freshest gouge (Figs. 13 and 15).

In addition, from the conventional logging curves, we can see that the borehole diameter is irregular from 585 to 590 m-depth, and decreasing from 591 to 594 m-depth (Fig. 3c). From 585 to 600 m-depth, there is a 0.15 °C temperature anomaly (Fig. 15a), a dramatic natural gamma ray increase from 60 API to ~90 API (Fig. 15b), an acoustic time increase from 60 μs/ft to >100 μs/ft (Fig. 15c), a minor negative anomaly of the self-potential (Fig. 15d), an apparent resistivity decrease from ~2000 Ωm to dozens of Ωm (Fig. 15e), and a high susceptibility at 590 m-depth (Fig. 15f).

From the borehole temperature measurement curves, one can see that there are three possibilities for the positive temperature anomaly peak within 15 m: 1) Friction along co-seismic fault yielded temperature rise and its effect still remained until the temperature was monitored. The residual frictional heat produced during the Chi-Chi earthquake remaining in the TCDP borehole is a good example (Kano et al., 2006). 2) There is a thermal anomaly at this depth due to fluid effects. 3) Thermal anomaly was caused by some radioactive elements within the rocks. If the temperature is measured again after a period of time, in general, the first kind of positive temperature anomaly peak becomes smaller while the latter two cases are constant. A year later, there were still temperature anomalies in the WFSD-1 borehole at the same depth, but the abnormal value decreased from 0.15 °C to 0.018 °C (Li et al., 2010b). Therefore, this is another good evidence that FZ590 most likely represents the Wenchuan earthquake fault zone, and that its PSZ is probably located close to 590 m-depth. Nevertheless, there is another possibility that the temperature fluctuation is caused by variation in thermal conductivity.

In FZ590 fault core (zone), there are many fault gouge layers (Fig. 13), but the darkest layer of gouge can only be seen at one location (589.17–589.25 m-depth), where it is the freshest (Figs. 13 and 15g), and where the magnetic susceptibility is the highest. The occurrence of this kind of gouge may be due to increasing magnetic mineral composition due to high temperature resulting from friction (Hirono et al., 2006, 2008; Pei, et al., 2010; Tanikawa et al., 2008). Taiwan's Chi-Chi earthquake produced only a 3 mm to 2 cm-thick gouge (Kuo et al., 2009, 2011; Ma et al., 2006). Therefore, the ~8 cm-thick black fresh gouge most probably not just results from the single Wenchuan earthquake.

We made continuous thin sections along the 589.04 to 589.34 m core segment containing the fresh gouge (Fig. 16) and analyzed its microstructure. Many fragments are observed in the core. Some calcite clasts and small veins (Fig. 16b) are present within the fresh gouge (outlined by yellow dotted lines in Fig. 16), while the segment in red dotted lines is darker and generally does not contain calcite (Fig. 16d, plane-polarized light). S-C fabrics and asymmetric rotational structures occur in the well-developed foliated gouge, showing the distinct shearing direction. In the whole section, only the segment in red dotted lines (~589.21 to 589.22 m) is fine, uniform and clean (Fig. 16d), where higher percentage of smectite (Si et al., 2010) can be a key evidence for locating the PSZ (Kuo et al., 2009, 2011). Therefore, the ~1 cm-thick layer (red dotted lines in Fig. 16d) most likely represents the PSZ of the Wenchuan earthquake where the slip plane can be observed.

Combining the boundary between the Neoproterozoic Pengguan complex and the late Triassic Xujiahe sedimentary rocks, as well as the logging data and microstructure features, the PSZ of the Wenchuan earthquake can preliminary be determined near 589 m-depth (~589.21 to 589.22 m), where ~1 cm thick fresh gouge was produced by the Wenchuan earthquake. The investigation of the surface rupture zone in the Hongkou outcrop area suggests that the width of the Wenchuan earthquake co-seismic surface slip zone was 2 to 3 mm (Lin, 2011) or 10–20 mm (Togo et al., 2011). Since the gouge from the surface rupture zone contained illite, chlorite but no smectite (Togo et al., 2011), it most likely indicates that it has been produced by former events, not just by the Wenchuan earthquake.

Now, we are able to calculate the dip angle around 600 m-depth, below the PSZ of the Wenchuan earthquake. If one draws a straight line from the location of the surface rupture to 589 m-depth in the borehole, we obtain a slip plane dip of 65°. Considering that the surface characteristics (dip angle of 75°–82°, Li et al., 2008, 2010a,b) might extend downward, we can infer an angle of ~62°. Consequently, the characteristics of the Wenchuan earthquake's PSZ are N305°–N317° with a dip angle of ~65° (FB showed in thick red solid line in Fig. 17).

The PSZ is tilted to cut through the whole Yingxiu–Beichuan fault zone if it is at 589 m-depth (thick red line FB in Fig. 17). At this point, we do not have enough evidence to determine the deformation process and fracture mechanism at 759 m-depth (thick red dashed line FA in Fig. 17) but detailed work including clay minerals and microstructure analysis are being performed to determine the Wenchuan earthquake PSZ orientation.

6.3. Fault activity

Fault gouge produced by fault activity is the key portion of a fault zone (Faulkner et al., 2010; Sibson, 2003) and is closely related to seismic events (Ma et al., 2006; Sibson, 1975). In other words, the thickness of the fault gouge is a function of the frequency of seismic events (Ma et al., 2006). Even though it can be affected by various factors such as seismic intensity, lithology of wall rocks and fluid characteristics, the fault gouge activated by a single seismic event is commonly from several millimeters to several centimeters large (Kuo et al., 2009; Ma et al., 2006; Sibson, 1975; Song et al., 2007). The fault gouge formed by the Chi-Chi earthquake (Mw 7.6) is only ~3 mm to 2 cm-thick (Kuo et al., 2009, 2011; Ma et al., 2006). Nevertheless, tens of centimeters to several meters-wide fault gouges might result from numerous large earthquakes. In WFSD-1 cores, just ~1 cm out of the 8 cm-thick black fresh fault gouge found in the FZ590 core is related to the Wenchuan earthquake.

In WFSD-1 cores, the fault gouge can be recognized in 10 out of 12 fault cores (or sub-fault zones), forming the Yingxiu–Beichuan fault (Table 1, Fig. 11), and shows dozens of layers with various thicknesses with a cumulative value that can be up to 3.79 m just in FZ590, similar to other thin gouge layers in the cores, indicating large historical seismic events. As shown in Fig. 16, the fault zone of the Wenchuan earthquake (FZ590) lies on top of the 10 fault cores of the Yingxiu–Beichuan fault zone, and the PSZ is represented by the thin ~1 cm-thick gouge at about 589 m-depth, although it does not correspond to the surface

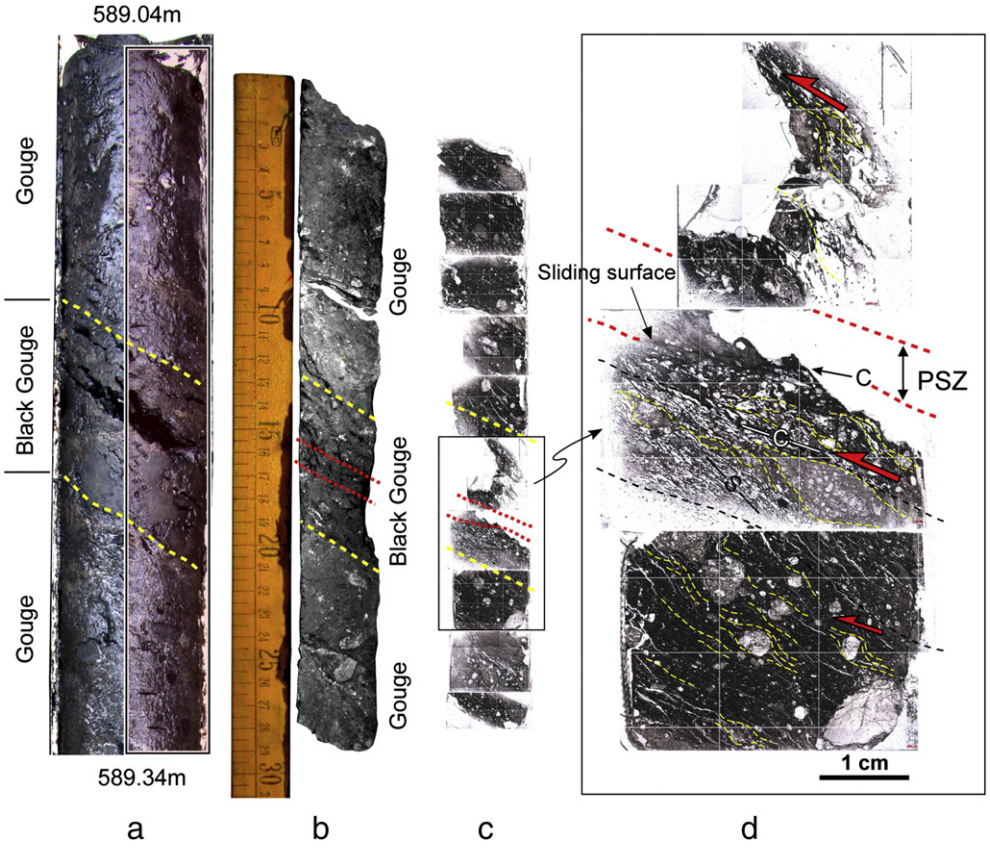

Fig. 16. Microstructure of fresh gouge in FZ590 of WFSD-1 cores. (a) The central part of the gouge is broken due to water loss and is located close to the slip plane. The pink area to the right is the location of thin sections; (b) the broken part shows the bands of calcite (white fragments). The section between red dotted lines is darker and generally without calcite; (c) the continuous thin sections (plane-polarized light) correspond to (b); (d) gouge micrograph (plane-polarized light). S-C fabrics occur in the foliated gouge. The PSZ of the Wenchuan earthquake is outlined by red dotted lines where fine and uniform grains as well as the slip plane can be observed.

location of the bottom of the Yingxiu–Beichuan fault zone and the surface rupture zone of the Wenchuan earthquake (Lin et al., 2010; Togo et al., 2011; Wang et al., 2010), suggesting an intense fault activity. The range of the fault zone bears certain relationship with seismicity frequency, and the history of the numerous earthquakes might be directly responsible for the uplift of the Longmenshan.

7. Conclusions

The Wenchuan earthquake Fault Scientific Drilling project (WFSD) provides a unique opportunity to investigate the faulting mechanism of the Wenchuan earthquake that struck the Longmenshan fault zone in 2008. The following conclusions have been obtained by analyzing the cores from the 1201 m-deep WFSD-1 borehole and interpreting the logging data.

(1) Three types of fault-related rocks are present in the WFSD-1 cores: fault gouge, cataclasite, and fault breccia. The core profile contains at least 12 subsidiary fault zones (fault cores), with 2 mm to 3.79 m-thick fault gouge, the latter coming from the FZ590 core and indicates long-term seismic activity in the region.
(2) The FZ590 core represents the boundary between the Neoproterozoic Pengguan complex (including pyroclastics, volcanic rocks, diorite and porphyrite) and the Late Triassic Xujiahe formation (including sandstone, siltstone, shale and liquid breccia).
(3) The Yingxiu–Beichuan fault zone is about ~100 m-wide from the distribution depths between 575.7 and 759 m with multiple fault cores in the WFSD-1 cores, and about ~190 m-wide measured from the outcrop and is restricted to the hanging wall.
(4) According to the logging data, fresh gouge appearance, high magnetic susceptibility values, and microstructure, FZ590 most likely represents the fault zone of the Wenchuan earthquake, and the Principle Slip Zone (PSZ), located at 589.21–589.22 m-depth, with ~1 cm-thick fresh fault gouge. The Wenchuan earthquake has a slip plane dip angle of ~65°, showing the high-angle thrust feature. The Yingxiu–Beichuan fault zone dips 68°–73° at or near the bottom of the fault zone, which is a different angle than the inferred co-seismic fault plane.
(5) The many fault gouges are very thick (85–379 cm) in the Yingxiu–Beichuan fault zone, the PSZ has ~1 cm-thick fault gouge resulting from the Wenchuan earthquake, which indicates intense fault activity, suggesting a correlation between the fault zone and the seismic event frequency. Numerous recurrent large earthquakes along the Longmenshan central fault yielded the Longmenshan uplift.

Acknowledgments

The authors thank Shiyou Hu, Wei Zhang, Jun Jia and Lasheng Fan of the Wenchuan Earthquake Fault Scientific Drilling Centre for their help. The authors also thank the field drilling workers and well logging by the 403 and 405 geological survey teams of the Sichuan Geology & Mineral Resources Bureau, respectively. We thank T. Shimamoto, Lu Yao and Yu Wang for helping us with reexamination of our fault-zone data. This work was supported by the "Wenchuan Earthquake Fault Scientific Drilling" of the National Science and Technology Planning Project. We also thank two anonymous reviewers for their comments which greatly improved this manuscript.

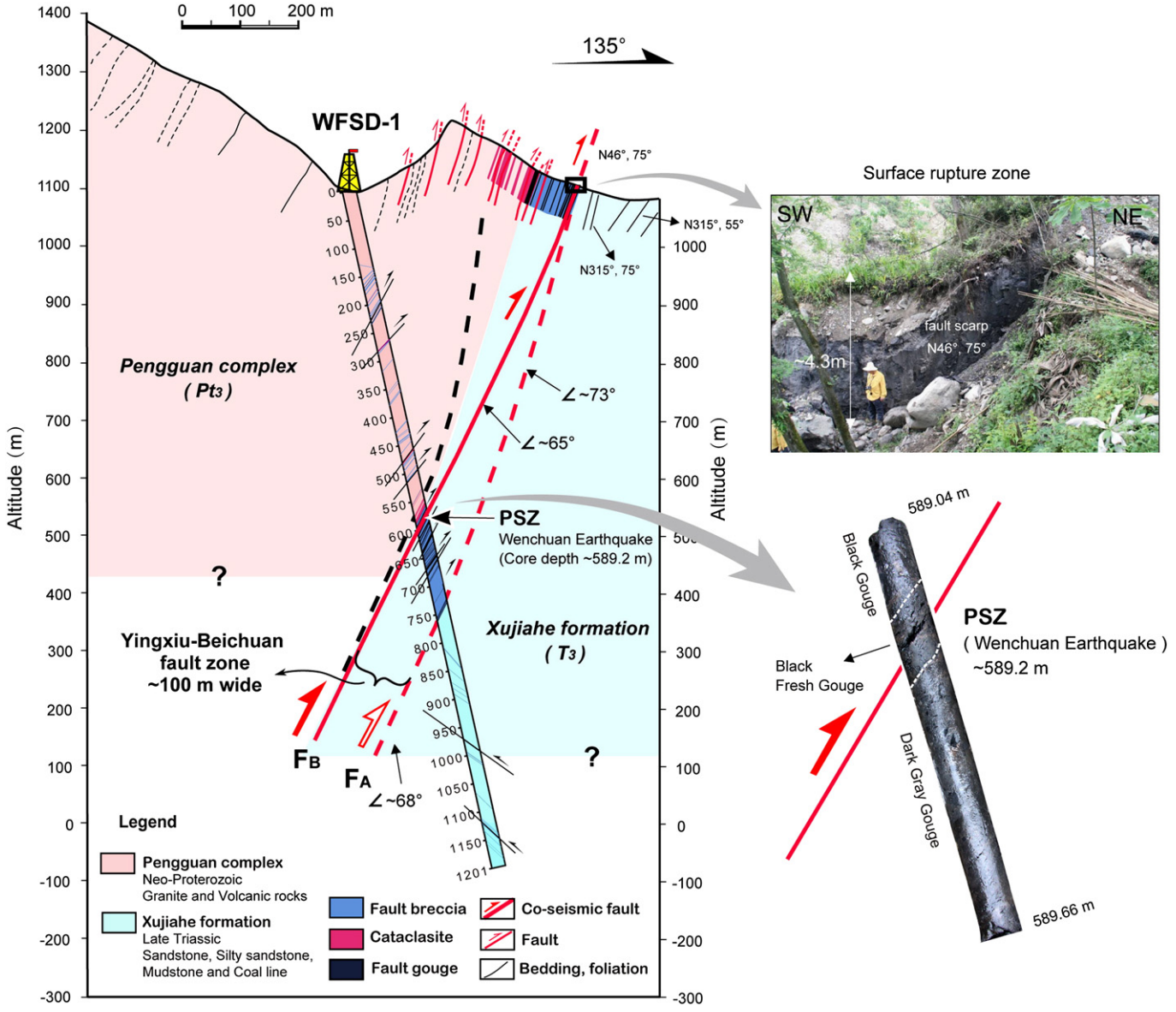

Fig. 17. Geologic cross-section across WFSD-1 drilling site of the 1200-m deep hole and co-seismic surface rupture zone of the Wenchuan earthquake. The width of the Yingxiu–Beichuan fault zone (consisting of cataclasite, fault breccia and fault gouge) is about 190 m at the outcrop. The surface rupture zone strikes N46°E and dips 75°NW at the bottom of the fault zone at the outcrop. FA: co-seismic fault inferred from the dip angle observed at the surface and joins to the bottom of the fault zone in WFSD-1 cores. FB: co-seismic fault inferred in this study (see text for details). The Yingxiu–Beichuan fault zone is about 100 m-wide in the WFSD-1 cores, similar to the 190 m-width of the fault zone at the outcrop. The dip angle of the Yingxiu–Beichuan fault zone is about 68°–73° at a depth of ~760 m.

Appendix A. Supplementary data

Supplementary data associated with this article can be found in the online version, at http://dx.doi.org/10.1016/j.tecto.2012.08.021. These data include Google maps of the most important areas described in this article.

References

Boullier, A.M., 2011. Fault-zone geology: lessons from drilling through the Nojima and Chelungpu faults. Geological Society, London, Special Publications 359, 17–37 http://dx.doi.org/10.1144/SP359.2.

Brodsky, E., Ma, K.F., Mori, J., Saffer, D.M., 2009. Rapid response fault drilling: past, present and future. Report of the ICDP/SCEC International Workshop of Rapid Response Fault Drilling. Tokyo, Japan, Nov. 17–19.

Burchfiel, B.C., Chen, Z.L., Liu, Y., Royden, L.H., 1995. Tectonics of the Longmen Shan and Adjacent Regions, Central China. International Geology Review 37 (8), 661–735.

Chengdu Institute of Technology, 1996. Geologic map of Dujiangyan (scale 1: 50000) (in Chinese).

Chester, F.M., Logan, J.M., 1986. Implications for mechanical properties of brittle faults from observations of the Punchbowl fault zone, California. Pure and Applied Geophysics 124, 79–106.

Chester, F.M., Friedman, M., Logan, J.M., 1985. Foliated cataclasites. Tectonophysics 111, 139–146.

Deng, Q.D., Chen, S.F., Zhao, X.L., 1994. Tectonics, seismicity, and dynamics of the Longmen Shan Mountains and its adjacent regions. Seismology and Geology 16 (4), 389–403 (in Chinese with English abstract).

Densmore, A.L., Ellis, M.A., Li, Y., Zhou, R.J., Hancock, G.S., Richardson, N., 2007. Active tectonics of the Beichuan and Pengguan faults at the eastern margin of the Tibetan Plateau. Tectonics 26, TC4005 http://dx.doi.org/10.1029/2006TC001987.

Faulkner, D.R., Rutter, E.H., 2003. The effect of temperature, the nature of the pore fluid, and subyield differential stress on the permeability of phyllosilicate-rich fault gouge. Journal of Geophysical Research - Solid Earth 108, B5.

Faulkner, D.R., Jackson, C.A.L., Lunn, R.J., Schlische, R.W., Shipton, Z.K., Wibberley, C.A.J., Withjack, M.O., 2010. A review of recent developments concerning the structure, mechanics and fluid flow properties of fault zones. Journal of Structural Geology 32, 1557–1575.

Feng, X.Y., 1997. The Paleoearthquakes in Xinjiang Region, China. Xinjiang Science and Sanitary Press, Urumqi . (in Chinese).

Fu, B.H., Shi, P.L., Wang, P., Li, Q., Kong, P., Zheng, G.D., 2009. Geometry and kinematics of the Wenchuan earthquake surface ruptures around the Qushan Town of Beichuan County, Sichuan: implications for mitigation of seismic and geologic

disasters. Chinese Journal of Geophysics 52 (2), 485–495 (in Chinese with English abstract).
Fu, B.H., Shi, P.L., Guo, H.D., Okuyama, S., Ninomiya, Y., Wright, S., 2011. Surface deformation related to the 2008 Wenchuan earthquake, and mountain building of the Longmen Shan, eastern Tibetan Plateau. Journal of Asian Earth Sciences 40 (4), 805–824.
Hirono, T., Ikehara, M., Otsuki, K., Mishima, T., Sakaguchi, M., Soh, W., Omori, M., Lin, W.R., Yeh, E.C., Tanikawa, W., Wang, C., 2006. Evidence of frictional melting from disk-shaped black material, discovered within the Taiwan Chelungpu fault system. Geophysical Research Letters 33, L19311 http://dx.doi.org/10.1029/2006GL027329.
Hirono, T., Fujimoto, K., Yokoyama, T., Hamada, Y., Tanikawa, W., Tadai, O., Mishima, T., Tanimizu, M., Lin, W.R., Soh, W., Song, S.R., 2008. Clay mineral reactions caused by frictional heating during an earthquake: an example from the Taiwan Chelungpu fault. Geophysical Research Letters 35, L16303 http://dx.doi.org/10.1029/2008GL034476.
Kano, Y., Mori, J., Fujio, R., Ito, H., Yanagidani, T., Nakao, S., Ma, K.F., 2006. Heat signature on the Chelungpu fault associated with the 1999 Chi-Chi, Taiwan earthquake. Geophysical Research Letters 33, L14306 http://dx.doi.org/10.1029/2006 GL026733.
Kuo, L.W., Song, S.R., Yeh, E.C., Chen, H.F., 2009. Clay mineral anomalies in the fault zone of Chelungpu Fault, Taiwan, and its implication. Geophysical Research Letters 36, L18306 http://dx.doi.org/10.1029/2009GL039269.
Kuo, L.W., Song, S.R., Huang, L., Yeh, E.C., Chen, H.F., 2011. Temperature estimates of coseismic heating in clay-rich fault gouges, the Chelungpu fault zones, Taiwan. Tectonophysics 502 (3–4), 315–327.
Li, Y., Hou, Z.J., Si, G.Y., Densmore, A.L., Zhou, R.C., Ellis, M.A., Li, Y.Z., Liang, X.Z., 2002. Cenozoic tectonic sequence and tectonic events at the eastern margin of the Qinghai-Tibet plateau. Geology in China 29 (1), 30–36 (in Chinese with English abstract).
Li, Y., Zhou, R.J., Densmore, A.L., Ellis, M.A., 2006. Geomorphic evidence for the late Cenozoic strike–slipping and thrusting in Longmen Mountain at the eastern margin of the Tibetan Plateau. Quaternary Sciences 26 (1), 40–51 (in Chinese with English abstract).
Li, H.B., Fu, X.F., Van der Word, J., Si, J.L., Wang, Z.X., Hou, L.W., Qiu, Z.L., Li, N., Wu, F.Y., Xu, Z.Q., Tapponnier, P., 2008. Co-seisimic surface rupture and dextral-slip oblique thrusting of the Ms 8.0 Wenchuan earthquake. Acta Geological Sinica 82 (12), 1623–1643 (in Chinese with English abstract).
Li, H.B., Si, J.L., Fu, X.F., Qiu, Z.L., Li, N., Van der Woerd, J., Pei, J.L., Wang, Z.X., Hou, L.W., Wu, F.Y., 2009. Co-seismic rupture and maximum displacement of the 2008 Wenchuan earthquake and its tectonic implications. Quaternary Sciences 29 (3), 387–402 (in Chinese with English abstract).
Li, H.B., Si, J.L., Pei, J.L., Fu, X.F., Wang, Z.X., Li, N., Hou, L.W., Wu, F.Y., Pan, J.W., 2010a. Surface rupture process of the Wenchuan earthquake (Ms 8.0). Quaternary Sciences 30 (4), 677–698 (in Chinese with English abstract).
Li, H., Xu, Z., Si, J., Pei, J., Li, T., Huang, Y., Wang, H., 2010b. Characteristics of the fault-related rocks, fault zone structures and the principal slip zone of the Wenchuan earthquake in WFSD drilling cores. American Geophysical Union, Fall Annual Meeting, San Francisco, T53E-02, Dec. 13–17.
Li, C.Y., Wei, Z.Y., Ye, J.Q., Han, Y.B., Zheng, W.J., 2010c. Amounts and styles of coseismic deformation along the northern segment of surface rupture, of the 2008 Wenchuan Mw 7.9 earthquake, China. Tectonophysics 491, 35–58.
Lin, A., 2011. Seismic slip recorded by fluidized ultracataclastic veins formed in a coseismic shear zone during the 2008 Mw 7.9 Wenchuan earthquake. Geology 39, 547–550 http://dx.doi.org/10.1130/G32065.1.
Lin, A., Chen, A., Liau, C.F., Lee, C.T., Lin, C.C., Lin, P.S., Wen, S.C., Ouchi, T., 2001. Frictional fusion due to coseismic landsliding during the 1999 Chi-Chi (Taiwan) M_L 7.3 earthquake. Geophysical Research Letters 28 (20), 4011–4014.
Lin, A., Maruyama, T., Kobayashi, K., 2007. Tectonic implications of damage zone-related fault-fracture networks revealed in drill core through the Nojima fault, Japan. Tectonophysics 443, 161–173.
Lin, A., Ren, Z.K., Kumahara, Y., 2010. Structural analysis of the coseismic shear zone of the 2008 Mw7.9 Wenchuan earthquake. Journal of Structural Geology 32, 781–791.
Liu, J., Zhang, Z.H., Wen, L., Sun, J., Xing, X.C., Hu, G.Y., Xu, Q., Tapponnier, P., Zeng, L.S., Ding, L., Liu, Y.L., 2008. The Ms 8.0 Wenchuan earthquake co-seismic rupture and its tectonic implications: an out of sequence thrusting event with slip partitioned on multiple faults. Acta Geologica Sinica 82 (12), 1707–1722 (in Chinese with English abstract).
Liu-Zeng, J., Wen, L., Sun, J., Zhang, Z.H., Hu, G.Y., Xing, X.C., Zeng, L.S., Xu, Q., 2010. Surficial Slip and Rupture Geometry on the Beichuan Fault near Hongkou during the Mw 7.9 Wenchuan Earthquake, China. Bulletin of the Seismological Society of America 100 (5B), 2615–2650.
Ma, Y.W., Wang, G.Q., Hu, X.W., 1996. Tectonic deformation of Pengguan complex as a nappe. Acta Geologica Sichuan 16 (2), 110–114 (in Chinese with English abstract).
Ma, K.F., Tanaka, H., Song, S.R., Wang, C.Y., Hung, J.H., Tsai, Y.B., Mori, J., Song, Y.F., Yeh, E.C., Soh, W., Sone, H., Kuo, L.W., Wu, H.Y., 2006. Slip zone and energetics of a large earthquake from the Taiwan Chelungpu-fault Drilling Project. Nature 444 (7118), 473–476.
Magloughlin, J.F., Spray, J.G., 1992. Frictional melting processes and products in geological materials: introduction and discussion. Tectonophysics 204 (3–4), 197–204.
Oshiman, N., Shimamoto, T., Takemura, K., Wibberley, C.A.J. (Eds.), 2001. Thematic issue: Nojima fault zone probe: Island Arc, 10, pp. 195–505.
Pei, J.L., Li, H.B., Sun, Z.M., Wang, H., Si, J.L., 2010. Fault slip in the Wenchuan earthquake fault zone — information from fault rocks with higher magnetic susceptibility. Quaternary Sciences 30 (4), 759–767 (in Chinese with English abstract).
Qiao, X.F., Guo, X.P., Li, H.B., Gou, Z.H., Su, D.C., Tang, Z.M., Zhang, W., Yang, G., 2012. Soft-sediment deformation in the Late Triassic and the Indosinian tectonic movement in Longmenshan. Acta Geologica Sinic 86 (1), 132–156 (in Chinese with English abstract).
Ran, Y.K., Shi, X., Wang, H., Chen, L.C., Chen, J., Liu, R.C., Gong, H., 2010. The maximum coseismic vertical surface displacement and surface deformation pattern accompanying the Ms 8.0 Wenchuan earthquake. Chinese Science Bulletin 55 (9), 841–850.
Si, J., Li, H., Song, S., Kuo, L., Pei, J., Wang, H., 2010. Clay mineral anomalies in WFSD drilling core and surface fault rocks and their significances. American Geophysical Union, Fall Annual Meeting. San Francisco, T51B-2044, Dec. 13–17, 2010.
Sibson, R.H., 1975. Generation of pseudotachylyte by ancient seismic faulting. Geophysical Journal of Royal Astronomical Society 43, 775–794.
Sibson, R.H., 1977. Fault rocks and fault mechanisms. Journal of the Geological Society 133 (3), 191–213.
Sibson, R.H., 2003. Thickness of the seismic slip zone. Bulletin of the Seismological Society of America 93 (3), 1169–1178.
Sichuan Bureau of Geology, 1975. Geologic map of Guangxian (scale 1: 200000) (in Chinese).
Song, S.R., Kuo, L.W., Yeh, E.C., Wang, C.Y., Hung, J.H., Ma, K.F., 2007. Characteristics of the lithology, fault-related rocks and fault zone structures in the TCDP Hole-A. Terrestrial Atmospheric and Oceanic Science 18, 243–269.
Tang, R.C., Han, W.B., 1993. Active Faults and Earthquake in Sichuan Province. Geological Press, Beijing, pp. 1–190 (in Chinese).
Tanikawa, W., Mishima, T., Hirono, T., Soh, W., Song, S.R., 2008. High magnetic susceptibility produced by thermal decomposition of core samples from the Chelungpu fault in Taiwan. Earth and Planetary Science Letters 272 (1–2), 372–381.
Theunissen, K., Smirnova, L., Dehandschutter, B., 2002. Pseudotachylytes in the southern border fault of the Cenozoic Intracontinental Teletsk basin (Altai, Russia). Tectonophysics 351 (1–2), 169–180.
Togo, T., Shimamoto, T., Ma, S.L., Wen, X.Z., He, H.L., 2011. Internal structure of Longmenshan fault zone at Hongkou outcrop, Sichuan, China, that caused the 2008 Wenchuan earthquake. Earthquake Science 24, 249–265 http://dx.doi.org/10.1007/s11589-011-0789-z.
Wang, E.Q., Meng, Q.R., 2008. Mesozoic and Cenozoic tectonic evolution of the Longmenshan fault belt. Science in China Series D: Earth Sciences 52 (5), 579–592.
Wang, E.Q., Meng, Q.R., Chen, Z.L., Chen, L.Z., 2001. Early Mesozoic left-lateral movement along the Longmen Shan fault belt and its tectonic implications. Earth Science Frontiers 8 (2), 375–384 (in Chinese with English abstract).
Wang, W.M., Zhao, L.F., Li, J., Yao, Z.X., 2008. Rupture process of the Ms 8.0 Wenchuan earthquake of Sichuan, China. Chinese Journal of Geophysics 51 (5), 1403–1410 (in Chinese with English abstract).
Wang, H., Li, H.B., Pei, J.L., Li, T.F., Huang, Y., Zhao, Z.D., 2010. Structural and lithologic characteristics of the Wenchuan earthquake fault zone and its relationship with the seismic activity. Quaternary Sciences 30 (4), 768–778 (in Chinese with English abstract).
Xu, Z.Q., Hou, L.W., Wang, Z.X., Fu, X.F., Wang, D.K., 1992. Orogenic processes of the Songpan Ganze orogenic belt of China. Geological Press, Beijing, pp. 1–190 (in Chinese).
Xu, Z.Q., Li, H.Q., Hou, L.W., Fu, X.F., Chen, W., Zeng, L.S., Cai, Z.H., Chen, F.Y., 2007. Uplift of the Longmen-Jinping orogenic belt along the eastern margin of the Qinghai-Tibet Plateau: large-scale detachment faulting and extrusion mechanism. Geological Bulletin of China 26 (10), 1262–1276 (in Chinese with English abstract).
Xu, Z.Q., Ji, S.C., Li, H.B., Hou, L.W., Fu, X.F., Cai, Z.W., 2008. Uplift of the Longmen Shan range and the Wenchuan earthquake. Episodes 31 (3), 291–301.
Xu, X.W., et al., 2008. The Ms 8.0 Wenchuan earthquake surface ruptures and its seismogenic structure. Seismology and Geology 30 (3), 597–629 (in Chinese with English abstract).
Xu, X.W., Wen, X.Z., Yu, G.H., Chen, G.H., Klinger, Y., Hubbard, J., Shaw, J.H., 2009. Coseismic reverse- and oblique-slip surface faulting generated by the 2008 Mw 7.9 Wenchuan earthquake, China. Geology 37 (6), 515–518.
Yan, Q.R., Hanson, A.D., Wang, Z.Q., Druschke, P.A., Yan, Z., Wang, T., Liu, D.Y., Song, B., Jian, P., Zhou, H., Jiang, C.F., 2004. Neoproterozoic Subduction and Rifting on the Northern Margin of the yangtze Plate, China: implications for Rodinia Reconstruction. International Geology Review 46 (9), 817–832.
Zhang, P.Z., Xu, X.W., Wen, X.Z., Ran, Y.K., 2008. Slip rates and recurrence intervals of the Longmen Shan active fault zone, and tectonic implications for the mechanism of the May 12 Wenchuan earthquake, 2008, Sichuan, China. Chinese Journal of Geophysics 51 (4), 1066–1073 (in Chinese with English abstract).
Zhang, Y., Feng, W.P., Xu, L.S., Zhou, C.H., Chen, Y.T., 2009. Spatio-temporal rupture process of the 2008 great Wenchuan earthquake. Science in China Series D: Earth Sciences 52 (2), 145–154.
Zhou, M.F., Yan, D.P., Wang, C.L., Qi, L., Kennedy, A., 2006. Subduction-related origin of the 750 Ma Xuelongbao adakitic complex (Sichuan Province, China): implications for the tectonic setting of the giant Neoproterozoic magmatic event in South China. Earth and Planetary Science Letters 248 (1–2), 286–300.
Zhou, R.J., Li, Y., Densmore, A.L., Ellis, M.A., He, Y.L., Wang, F.L., Li, X.G., 2006. Active tectonics of the eastern margin of the Tibet Plateau. Journal of Mineralogy and Petrology 26 (2), 40–51 (in Chinese with English abstract).
Zoback, M.D., Hickman, S., Ellsworth, W., 2007. The Role of Fault Zone Drilling. Geophysics 4, 649–674.